UNCLASSIFIED

SECURITY CLASSIFICATION OF THIS PAGE *(When Data Entered)*

REPORT DOCUMENTATION PAGE		READ INSTRUCTIONS BEFORE COMPLETING FORM
1. REPORT NUMBER NORDA Technical Note 92	2. GOVT ACCESSION NO.	3. RECIPIENT'S CATALOG NUMBER
4. TITLE *(and Subtitle)* Test and Evaluation of an Operationally Capable Synoptic Upper-Ocean Forecast System		5. TYPE OF REPORT & PERIOD COVERED 6. PERFORMING ORG. REPORT NUMBER
7. AUTHOR(s) R. Michael Clancy Paul J. Martin Steve A. Piacsek Kenneth D. Pollak		8. CONTRACT OR GRANT NUMBER(s)
9. PERFORMING ORGANIZATION NAME AND ADDRESS Naval Ocean Research and Development Activity NSTL Station, MS 39529		10. PROGRAM ELEMENT, PROJECT, TASK AREA & WORK UNIT NUMBERS
11. CONTROLLING OFFICE NAME AND ADDRESS		12. REPORT DATE April 1981 13. NUMBER OF PAGES 69
14. MONITORING AGENCY NAME & ADDRESS*(if different from Controlling Office)*		15. SECURITY CLASS. *(of this report)* Unclassified 15a. DECLASSIFICATION/DOWNGRADING SCHEDULE

16. DISTRIBUTION STATEMENT *(of this Report)*

Unlimited

17. DISTRIBUTION STATEMENT *(of the abstract entered in Block 20, if different from Report)*

18. SUPPLEMENTARY NOTES

19. KEY WORDS *(Continue on reverse side if necessary and identify by block number)*

Ocean Analysis
Ocean Prediction
Ocean Forecast Model
Ocean Thermal Structure
Oceanic Mixed Layer
Ocean Circulation
Hydroacoustics
Forecast Verification

20. ABSTRACT *(Continue on reverse side if necessary and identify by block number)*

This paper describes the first generation of operationally capable synoptic upper-ocean forecast models implemented at the U.S. Navy's Fleet Numerical Oceanography Center via the Thermodynamical Ocean Prediction System (TOPS), and discusses potential uses for their output products. Several examples of one-dimensional verification of the turbulence parameterization scheme currently used in TOPS are presented and discussed. In addition, formalism for large-scale synoptic verification of short-term ocean thermal predictions is developed and applied to a test and evaluation of TOPS that was carried

DD FORM 1 JAN 73 1473 EDITION OF 1 NOV 65 IS OBSOLETE
S/N 0102-014-6601

UNCLASSIFIED

SECURITY CLASSIFICATION OF THIS PAGE *(When Data Entered)*

out using operational data from the fall of 1980. Results from this 45-day testing period indicate that TOPS can routinely forecast large-scale sea surface temperature changes over periods of several days with a useful level of skill. This marks the practical beginning of operational synoptic ocean prediction.

AN (1) AD-A098 908
FG (2) 040200
FG (2) 120300
FG (2) 200400
CI (3) (U)
CA (5) NAVAL OCEAN RESEARCH AND DEVELOPMENT ACTIVITY NSTL STATION MS
TI (6) Test and Evaluation of an Operationally Capable Synoptic Upper-Ocean Forecast System.
DN (9) Technical note,
AU (10) Clancy,R. Michael
AU (10) Martin,Paul J.
AU (10) Piacsek,Steve A.
AU (10) Pollak,Kenneth D.
RD (11) Apr 1981
PG (12) 73p
RS (14) NORDA-TN-92
RC (20) Unclassified report
DE (23) *Synoptic meteorology, *Ocean surface, *Mathematical prediction, Boundary value problems, Thermal properties, One dimensional, Numerical analysis, Advection, Turbulent boundary layer, Real time, Finite difference theory, Correlation techniques, Error analysis, Thermal analysis, Ocean models
DC (24) (U)
ID (25) TOPS(Thermodynamical Ocean Prediction System), Initial value problems
IC (26) (U)
AB (27) This paper was prepared for the Ocean Prediction Workshop held at the Naval Postgraduate School, 29 April through 2 May 1981. It describes the first generation of operationally capable synoptic upper-ocean forecast models implemented at Fleet Numerical Oceanography Center via the Thermodynamical Ocean Prediction System (TOPS), and discusses potential uses for their output products. Several examples of one-dimensional verification of the turbulence parameterization scheme currently used in TOPS are presented and discussed. In addition, formalism for large-scale synoptic verification of short-term ocean thermal predictions is developed and applied to a test and evaluation of TOPS that was carried out using operational data from the fall of 1980. Results from this 45-day testing period indicate that TOPS can routinely forecast large-scale sea surface temperature changes over periods of several days with a useful level of skill. This marks the practical beginning of operational synoptic ocean prediction. (Author)
AC (28) (U)
DL (33) 01
CC (35) 392773

NORDA Technical Note 92

Naval Ocean Research
and Development Activity
NSTL Station, Mississippi 39529

Test and Evaluation of an Operationally Capable Synoptic Upper-Ocean Forecast System

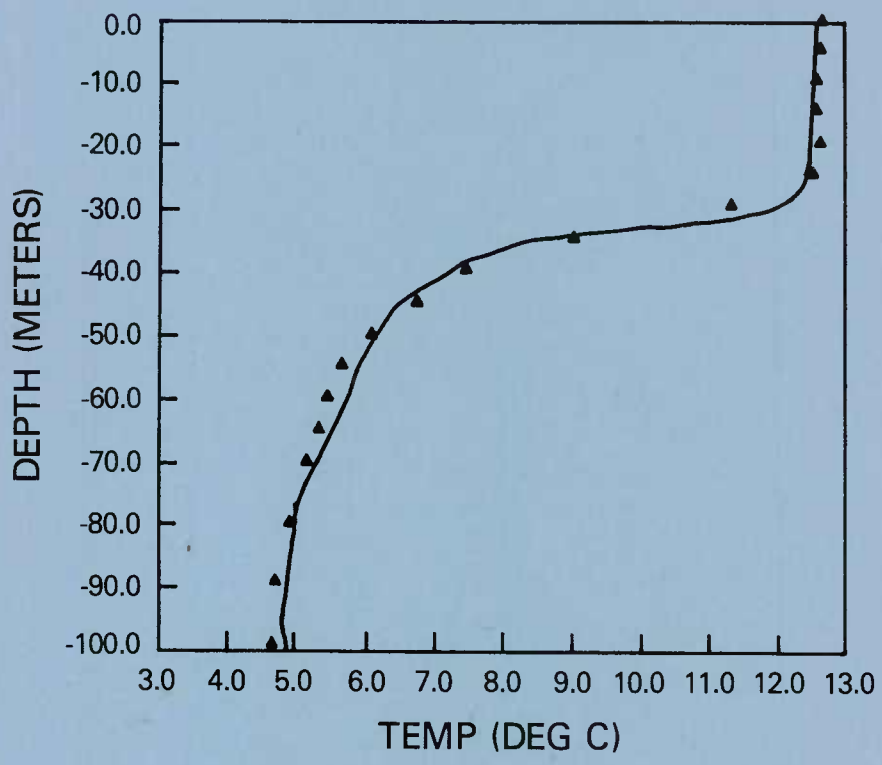

R. Michael Clancy
Paul J. Martin
Steve A. Piacsek

Numerical Modeling Division
Ocean Science and Technology Laboratory

Kenneth D. Pollak

Data Integration Department
Fleet Numerical Oceanography Center
Monterey, CA 93940

MARCH 1981

ABSTRACT

This paper was prepared for the Ocean Prediction Workshop held at the Naval Postgraduate School, 29 April through 2 May 1981. It describes the first generation of operationally capable synoptic upper-ocean forecast models implemented at Fleet Numerical Oceanography Center via the Thermodynamical Ocean Prediction System (TOPS), and discusses potential uses for their output products. Several examples of one-dimensional verification of the turbulence parameterization scheme currently used in TOPS are presented and discussed. In addition, formalism for large-scale synoptic verification of short-term ocean thermal predictions is developed and applied to a test and evaluation of TOPS that was carried out using operational data from the fall of 1980. Results from this 45-day testing period indicate that TOPS can routinely forecast large-scale sea surface temperature changes over periods of several days with a useful level of skill. This marks the practical beginning of operational synoptic ocean prediction.

CONTENTS

ILLUSTRATIONS

I. INTRODUCTION

The evolution of environmental parameters in the upper ocean has important impacts on the performance of weapons systems, acoustic surveillance capabilities, non-acoustic ASW, search and rescue planning, and other aspects of modern naval operations. Thus, the Navy requires an operational capability to accurately represent the present and future state of the oceanic environment.

Because of its influence on acoustics, upper ocean thermal structure is a particularly important environmental parameter. Currently, the Navy must rely on climatological data bases combined with analyses of extremely sparse XBT and surface ship observations to provide ocean thermal information. The success of these products has been quite limited, however, primarily because ocean thermal structure exhibits considerable variability about the climatological state, and the traditional observing systems are incapable of synoptically resolving this variability on the time and space scales required by the Navy. Maximum use of satellite data, blended with *in situ* observations via sophisticated analysis techniques such as optimum interpolation, shows promise of improving the situation. In addition, numerical ocean prediction models, combined with the sophisticated analysis techniques, are powerful tools for improving the Navy's operational knowledge of the environment. The fundamental idea behind this approach is to solve the physical equations of an ocean prediction model to impose dynamical self-consistency on the available data bases and thereby gain an improved representation of oceanic variability.

The Naval Ocean Research and Development Activity (NORDA) has been tasked with advanced development, testing, and reprogramming of numerical ocean analysis and prediction models for operational use at the Navy's Fleet Numerical Oceanography Center (FNOC). In support of these efforts, an elaborate software product, designated as Thermodynamical Ocean Prediction System (TOPS), has been developed. TOPS is a flexible and well-documented framework for operational implementation of upper-ocean forecast models at FNOC. It has been optimized for execution on the FNOC computers and installed on the FNOC operational program library. TOPS is interfaced with the Navy's operational environmental data base and was developed as a part of the Navy's Automated Environmental Prediction System (AEPS). In this paper we will

(1) define exactly what types of models are implemented via TOPS, (2) note uses for TOPS output products, (3) present results from the formal FNOC test and evaluation of the first version of TOPS, and (4) discuss the relationship between TOPS and future NORDA-produced operational ocean products.

II. MODELS IMPLEMENTED VIA TOPS

A. BASIC CHARACTERISTICS

Models that can be implemented via TOPS are best described as "NX1-D" or "Synoptic Mixed-Layer" Models. Several characteristics distinguish them. First of all, they include a detailed treatment of thermodynamics and mixed-layer physics, since prediction of changes in the thermal structure of the upper ocean is their primary objective. Furthermore, they predict these changes on a three-dimensional grid, even though fully three-dimensional processes are not included in their formulations.

Since the upper ocean is very much an atmospherically forced system, atmospheric predictions are required to drive these models, and their skill is closely related to that of the atmospheric models that generate these predictions. In addition, the time period over which deterministic real-time ocean forecasts can be made with these models is limited by the period over which the atmospheric forecasts are valid.

Finally, an extremely important characteristic of the synoptic mixed-layer models is that they neglect the pressure gradient terms in the momentum equations. This differentiates these models from fully hydrodynamical/thermodynamical models which retain these terms. Neglect of pressure effects makes initialization and updating of these models from operationally available analyses of sparse data practical, since it eliminates the possibility of spurious wave motions being excited by dynamically imbalanced initial states. Of course, neglect of the pressure gradient terms also eliminates any treatment of phenomena that are essentially hydrodynamical rather than thermodynamical in nature. For example, formation, movement, and decay of mesoscale eddies, meanderings of the Gulf Stream, and the downward propagation of internal waves are all important oceanic processes that are not dynamically represented in the TOPS models.

B. NON-ADVECTIVE AND ADVECTIVE FORMULATIONS

Two basic types of synoptic mixed-layer formulation are available in TOPS: non-advective and advective.

In the non-advective formulation, the only physical processes included are vertical mixing, radiation, and planetary rotation. The conservation equations for temperature, salinity, and momentum in this model are

$$\frac{\partial \bar{T}}{\partial t} = \frac{\partial}{\partial z}\left(\overline{-w'T'} + \nu\frac{\partial \bar{T}}{\partial z}\right) + \frac{1}{\rho_w c}\frac{\partial \bar{F}}{\partial z}\ , \tag{1}$$

$$\frac{\partial \bar{S}}{\partial t} = \frac{\partial}{\partial z}\left(\overline{-w'S'} + \nu\frac{\partial \bar{S}}{\partial z}\right)\ , \tag{2}$$

$$\frac{\partial \bar{u}}{\partial t} = f\bar{v} + \frac{\partial}{\partial z}\left(\overline{-w'u'} + \nu\frac{\partial \bar{u}}{\partial z}\right) - D\bar{u}\ , \tag{3}$$

$$\frac{\partial \bar{v}}{\partial t} = -f\bar{u} + \frac{\partial}{\partial z}\left(\overline{-w'v'} + \nu\frac{\partial \bar{v}}{\partial z}\right) - D\bar{v}\ , \tag{4}$$

where T is the temperature, S the salinity, u and v the x- and y-components of the current velocity (x and y horizontal coordinates relative to the grid), w the z-component of the current velocity, F the downward flux of solar radiation, D a damping coefficient, ν a diffusion coefficient, f the Coriolis parameter, t the time and z the vertical coordinate (positive upward from sea surface). Ensemble means are denoted by $(\bar{\ })$ and primes indicate departure from these means. Thus, for example, the quantity $\overline{w'S'}$ represents the vertical eddy (i.e., turbulent) flux of salinity.

The terms involving the damping coefficient D in (3) and (4) represent the drag force caused by the stress at the base of the mixed layer associated with the

propagation of internal wave energy downward and away from the wind-forced region (e.g., Pollard and Millard, 1970). As discussed by Niiler and Kraus (1977), this drag force can contribute to the relatively fast attenuation of inertial oscillations observed in the mixed layer. The terms involving ν in equations (1)-(4) account for very weak "background" eddy diffusion (due to intermittent breaking of internal waves, for example) that exists even below the mixed layer.

The purely one-dimensional physics of the non-advective formulation is capable of representing a significant part of the upper ocean's thermal response to strong atmospheric forcing on time scales of several days and space scales of several hundred kilometers (e.g., Camp and Elsberry, 1978; Clancy and Martin, 1981). In addition, this type of model is advantageous in that it requires minimal core storage in the computer, since gridpoints are not coupled horizontally.

In the advective formulation, horizontal and vertical advection and horizontal diffusion of temperature and salinity are included in addition to the radiative and vertical mixing processes of the non-advective model. As a result, the conservation equations for temperature and salinity become

$$\frac{\partial \bar{T}}{\partial t} = \frac{\partial}{\partial z}\left(\overline{-w'T'} + \nu\frac{\partial \bar{T}}{\partial z}\right) + \frac{1}{\rho_w c}\frac{\partial \bar{F}}{\partial z} - \frac{\partial}{\partial x}(u_a\bar{T}) - \frac{\partial}{\partial y}(v_a\bar{T}) - \frac{\partial}{\partial z}(w_a\bar{T}) + A\left(\frac{\partial^2 \bar{T}}{\partial x^2} + \frac{\partial^2 \bar{T}}{\partial y^2}\right), \tag{5}$$

and

$$\frac{\partial \bar{S}}{\partial t} = \frac{\partial}{\partial z}\left(\overline{-w'S'} + \nu\frac{\partial \bar{S}}{\partial z}\right) - \frac{\partial}{\partial x}(u_a\bar{S}) - \frac{\partial}{\partial y}(v_a\bar{S}) - \frac{\partial}{\partial z}(w_a\bar{S}) + A\left(\frac{\partial^2 \bar{S}}{\partial x^2} + \frac{\partial^2 \bar{S}}{\partial y^2}\right), \tag{6}$$

where u_a, v_a and w_a are the x-, y-, and z-components of the advection current and A is a spatially variable horizontal eddy diffusion coefficient calculated in the manner of Haney (1974). Definitions for the remaining symbols can be found either in the earlier discussion or in the Appendix.

As before, horizontal pressure gradients and horizontal advection and diffusion are neglected in the momentum equations. Therefore, these equations still take the form of Equations (3) and (4) of the non-advective model.

Inclusion of advection in this formulation allows the model to handle the longer time scales (i.e., weeks to months) more accurately than the non-advective model. Since gridpoints are coupled horizontally in the advective formulation, however, this type of model requires a substantial amount of core storage.

In the context of operations at FNOC, the advective model is designed to execute on the CYBER 203 computer as the primary model in TOPS. The non-advective model is programmed to execute either on the CYBER 175 or on one of the 6500's at FNOC and serve as a back-up model to be run in the event that the CYBER 203 is down.

C. GRID AND FINITE DIFFERENCE SCHEME

The vertical grid used in TOPS, on which $\overline{T}$, $\overline{S}$, $\overline{u}$, and $\overline{v}$ are defined, consists of 17 levels between the surface and 500 m depth and is shown in Figure 1. The vertical eddy fluxes and w_a are defined at depths midway between those for which temperature, salinity, and momentum are defined.

For the horizontal representation in TOPS, $\overline{T}$, $\overline{S}$, $\overline{u}$, and $\overline{v}$ are defined at the points of the standard FNOC 63 x 63 Northern Hemisphere Polar Stereographic Grid which is shown in Figure 2. This grid is true at 60°N where the spacing is 381 km. In the tropics, the spacing is of the order of 200 km.

In the advective model, w_a is also defined on this grid, but u_a and v_a are staggered with respect to these points. Figure 3 shows the basic elements of the resulting grid system.

The vertical eddy flux terms in equations (1)-(6) are differenced backward in time. The Coriolis and vertical advection terms are differenced trapezoidal in time, and all other terms are differenced forward in time. All spatial derivatives are centered in space. See Clancy (1981) for an analysis of the numerical stability of the advective model.

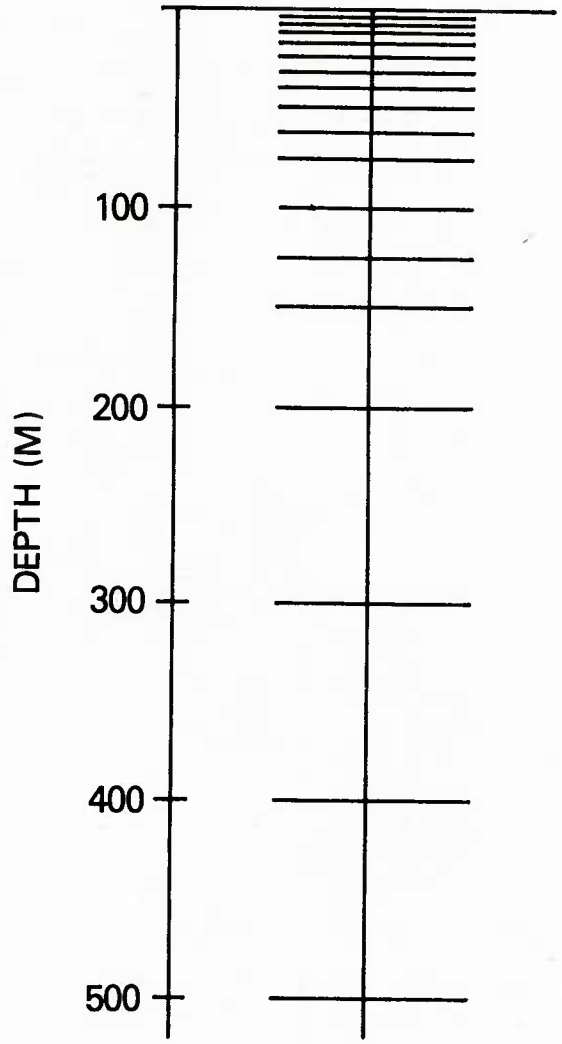

Figure 1. Vertical grid utilized by TOPS. The quantities $\overline{T}$, $\overline{S}$, $\overline{u}$, $\overline{v}$, u_a and v_a are defined at the depths indicated in the figure. All turbulence quantities and w_a are defined at depths midway between those shown in the figure.

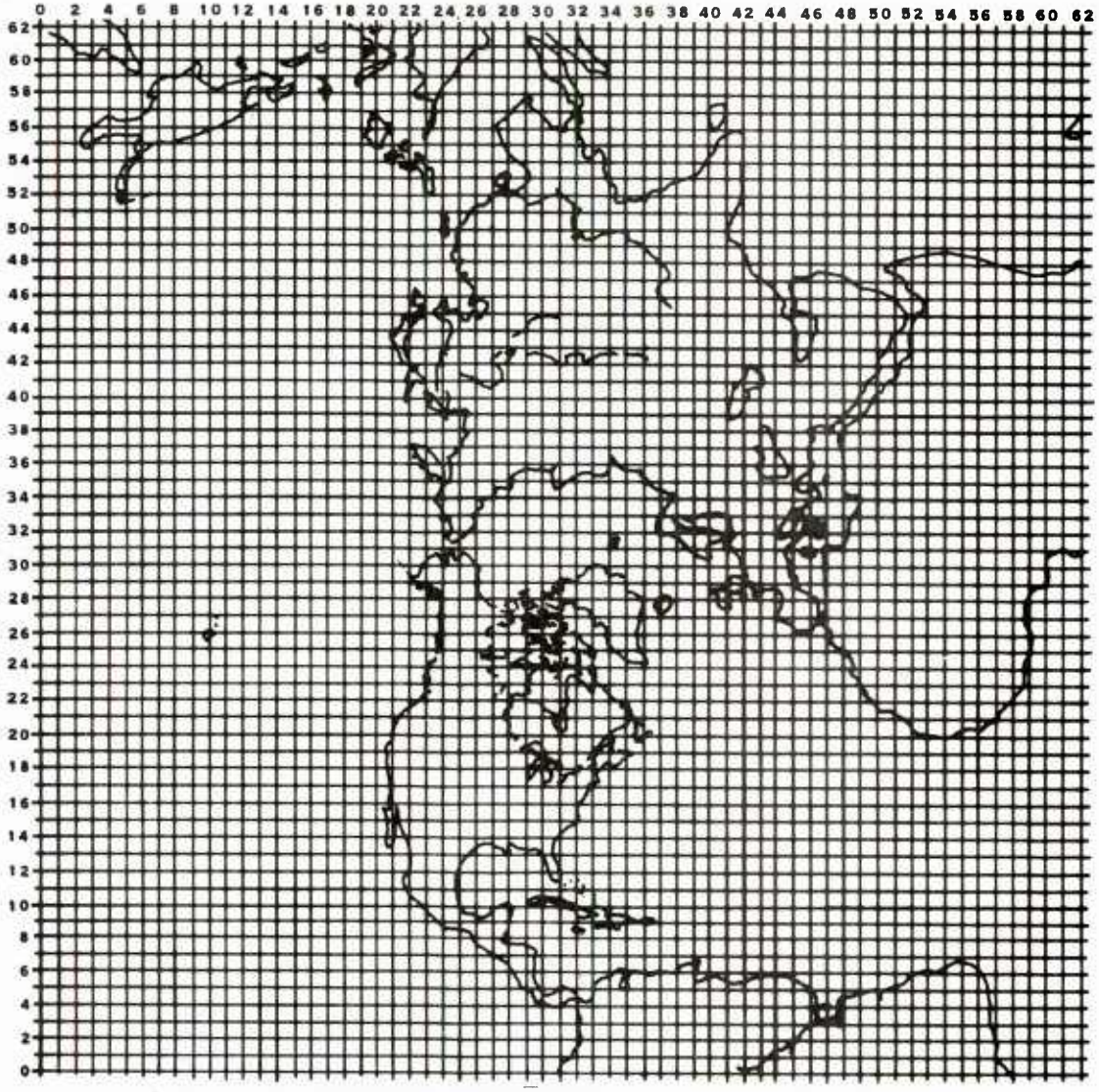

Figure 2. Standard 63 x 63 Northern Hemisphere Polar Stereographic Grid on Which $\overline{T}$, $\overline{S}$, $\overline{u}$, $\overline{v}$, and w_a are defined.

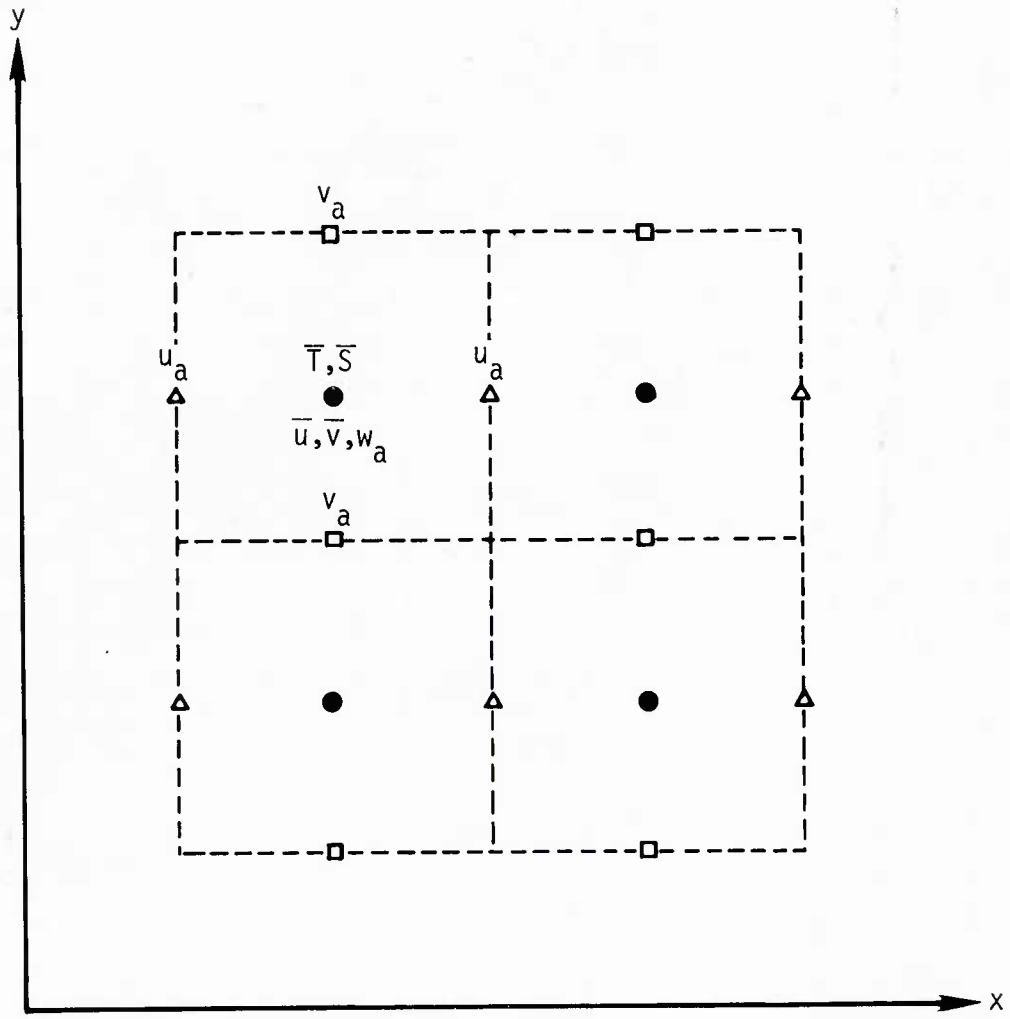

Figure 3. Staggered grid system used in the advective model. The quantities $\overline{T}$, $\overline{S}$, $\overline{u}$, $\overline{v}$, and w_a are defined at the points denoted ●, which correspond to the points in the standard FNOC 63 x 63 Northern Hemisphere Polar Stereographic Grid. The quantity u_a is defined at points denoted by △, and v_a is defined at points denoted by □. The interpolated climatological density field and the geostrophic stream function are defined at the corners of the dashed-line boxes.

D. INITIAL AND BOUNDARY CONDITIONS

It is important to emphasize that all data fields required by TOPS are generated operationally at FNOC. Thus, TOPS is capable of producing real-time forecasts on a routine basis.

Specifically, the initial temperature field for these forecasts is provided by the Expanded Ocean Thermal Structure (EOTS) Analysis (see Naval Air Systems Command Report 50-1G-522; Mendenhall et al., 1978; Holl et al., 1979). Briefly, this system is a successive corrections type of objective analysis scheme which contains no explicitly modeled physics and is based entirely on standard information blending concepts. The primary mixed-layer depth, temperatures at fixed levels, and temperatures at "floating" levels that move up and down with the primary layer depth for adequate resolution of the thermocline are produced. The analysis is updated every 24 hours with roughly 150 new XBT observations and 1500 new surface ship observations. Since information is blended vertically as well as horizontally, the sea-surface temperature observations contribute information to the subsurface thermal analysis. In data-void regions, the analyzed thermal field remains very near a state determined by a daily interpolation of monthly climatology (see Weigle and Mendenhall, 1974).

Salinity is included in TOPS because it makes an important contribution to the density stratification in some regions and thereby affects the vertical turbulent mixing (e.g., Miller, 1976; Price, 1979). Since salinity observations are not routinely made, however, a synoptic analysis for salinity is not available. Consequently, below the mixed layer (as determined by the initial temperature profile), the initial salinity is given by a daily interpolation of monthly climatology, while in the mixed layer it is adjusted slightly from climatology such that the initial density stratification is neutral there.

To initialize the momentum field in a "cold start" (i.e., in a situation where there is no prior momentum information available), the current is set to zero below the mixed layer and equal to the steady-state solution of (3) and (4) (subject to the initial wind stress) in the mixed layer. From this point on in a sequence of daily forecast runs, the initial momentum field is given by the 24-hour forecast momentum field calculated by the previous day's run. Thus, the momentum field is

integrated forward in time day-by-day until hardware failures or other difficulties necessitate another cold start.

The upper boundary conditions for the temperature, salinity, and momentum conservation equations are provided by surface fluxes that are forecast out to a period of 72 hours twice a day by the FNOC PE and PBL models (see Kesel and Winninghoff, 1972; Mihok and Kaitala, 1976; Naval Air Systems Command Report 50-1G-522). The lower boundary conditions for these equations are provided by holding the temperature, salinity, and momentum constant at the lower boundary of the model during each forecast run.

Because there are no horizontal exchanges of heat and salinity in the non-advective model, no lateral boundary conditions are required in that formulation. In the advective model, the normal component of the advection current and the normal derivatives of $\overline{T}$ and $\overline{S}$ are taken to be zero at land-sea boundaries. Thus, no advection or diffusion of temperature or salinity is allowed across these boundaries. In addition, the normal derivatives of $\overline{T}$ and $\overline{S}$ on the outer boundary surrounding the forecast domain (i.e., one-half grid space outside of the 63x63 grid) are assumed to be zero, which implies no diffusion of heat and salinity into or out of the domain. See Clancy and Martin (1979) for a more detailed discussion of the initial and boundary conditions used in TOPS.

E. TURBULENCE PARAMETERIZATION SCHEME

Modeling of the oceanic mixed layer is intrinsically linked to parameterization of turbulent processes and, consequently, is a difficult problem. Nevertheless, studies conducted in the past decade have shown that the state of the mixed layer is highly predictable, compared to other geophysical phenomena, with a variety of one-dimensional models.

In the present version of TOPS we use the turbulence parameterization scheme of Mellor and Durbin (1975) (which is essentially the Level-2 Scheme of Mellor and Yamada, 1974) to predict the vertical eddy flux terms in equations (1)-(6). In this turbulence model, the increase in potential energy during mixed-layer deepening due to the buoyancy flux at the layer base is balanced locally by mean flow shear generation minus viscous dissipation of turbulent kinetic energy. In this respect, its energetics are essentially the same as those of Pollard et al. (1973) and Thompson (1976).

We chose the Mellor-Durbin Scheme for use in TOPS because (1) it is widely used, (2) it has been tested successfully on time scales ranging from diurnal to annual in a number of studies, and, (3) it is of an appropriate level of complexity to be used in a first-generation operational model. We are not uniformly pleased with the performance of this scheme, however, and maintain an ongoing research effort at NORDA to test other schemes as a possible replacement for it. Turbulence models presently being considered in this regard are those of Garwood (1977), Vager and Zilitinkevich (1968), and several models currently under development at NORDA. Note that TOPS has been designed in a highly modular fashion so that implementation of new turbulence parameterization schemes can be accomplished with a minimum of effort.

F. CALCULATION OF THE ADVECTION CURRENT

The current used to advect temperature and salinity in the advective model is given by

$$u_a = u_i + u_g^* \tag{7}$$

$$v_a = v_i + v_g^* \tag{8}$$

$$w_a = w_i \tag{9}$$

where u_i and v_i are the x- and y-components of the instantaneous Ekman plus inertial current, w_i is the vertical and component of the current resulting from the divergence of u_i and v_i, and u_g^* and v_g^* are the x- and y-components of a non-divergent geostrophic velocity field determined from a climatological data base. The quantities u_i, v_i, and w_i are obtained by interpolating $\bar{u}$ and $\bar{v}$ to the staggered grid each time step of the integration (see Figure 3). The components of the geostrophic current are updated monthly by integrating the thermal wind equations upward from a latitude-dependent level of no motion using FNOC climatological temperature and salinity fields and then solving a stream function-vorticity equation to eliminate the horizontal divergence. This last step is necessary because the vertical motion field resulting from the divergence of the "raw" geostrophic currents proves to be excessively noisy. For details, see Clancy and Martin (1979).

Although the simplified treatment of geostrophic currents outlined above is adequate to account for the gross features of the large-scale oceanic gyres and

equatorial current systems, it is considered only an interim solution to the problem of providing geostrophic advection currents for TOPS. A potentially better solution to this problem is to use the World Ocean Primitive Equation Model presently under development at NORDA (see Section V) to supply these currents. This upgrade of the System will probably be accomplished in either 1982 or 1983.

III. USES FOR TOPS

There are many uses for information generated by TOPS, but in this paper we will concern ouselves only with those applications which are expected to be of direct use to the Navy. These applications fall basically into three categories: (1) improving the Navy's capability to synoptically analyze the existing thermal structure of the upper ocean, (2) providing the Navy with a real-time forecast capability for changes in upper ocean thermal structure on the time scale that atmospheric forecasts are valid, and (3) supplying the Navy with real-time information on the synoptic distribution of Ekman and inertial currents in the surface mixed layer.

A. USE OF TOPS IN OCEAN THERMAL ANALYSIS

Of the applications mentioned above, use of TOPS to improve ocean thermal analysis capabilities is probably the most important. To illustrate this, we consider the EOTS analysis currently in operation at FNOC. This system uses a forecast of adjustment toward climatology to generate the first-guess field (i.e., the best estimate of the field before the new data is assimilated) for the daily ocean thermal analysis. Consequently, in data-sparse regions, the analyzed thermal field stays very near a climatological state. This heavy reliance on climatology, however, is probably not the best approach. For example, as noted by Strong and Pritchard (1980), the NOAA Global Operational Sea Surface Temperature Computation (GOSSTCOMP) product was significantly improved when the climatological temperature field was dropped as a first-guess field in data-void areas.

This is not surprising since the thermal structure of the upper ocean does not, in general, follow the daily climatological trend. Instead, the mixed layer is characterized, broadly speaking, by relatively long periods of little or no change (other than diurnal), punctuated by rather dramatic warming and shallowing or cooling and deepening "events" associated with the passage of synoptic-scale weather patterns (e.g., Elsberry and Camp, 1978; Elsberry and Raney, 1978). Stated

succinctly, the variance of upper ocean thermal structure about the climatological mean is large.

An example of this is given by Figure 4, which shows a prediction of mixed layer depth at Ocean Station November (30°N, 140°W) during 1961 by the Mellor-Durbin Model. This prediction was forced with the standard meteorological observations made at the ocean station, and considerable variability is evident on the diurnal and synoptic-weather time scales. A climatology, no matter how good it is, will miss this variability. In addition, the predominance of variability on these time scales makes issuance of an objective ocean thermal analysis on a monthly or even weekly basis an inadequate approach (see also Figure 13).

Another important phenomenon illustrated by Figure 4 is that of spring transition of the mixed layer. This refers to the rapid and irreversible shallowing of the mixed layer from the deep wintertime regime to the shallow summertime regime, which occurs near the middle of April in this case. The transition occurs abruptly in response to an extended period of weak winds and strong surface heating. The actual date of transition is subject to the vagaries of developing springtime weather patterns and, thus, can exhibit departures on the order of plus or minus one month from climatology (see Elsberry and Garwood, 1978). Furthermore, if the transition occurs earlier than usual, then the heat supplied to the upper ocean during the early part of the heating season will be put into an anomalously shallow layer. This will tend to produce an anomalously warm summertime mixed layer and strong thermocline gradient. Similarly, if the transition occurs later than usual, an anomalously cool summertime mixed layer and weak thermocline gradient will tend to develop. Thus, heavy reliance on climatology in an ocean thermal analysis can lead to severe shortcomings in the spring and summer due to this phenomenon.

In addition, since the low-frequency cutoff for acoustic waves ducted in the mixed layer is proportional to mixed layer depth to the minus three halves power, spring transition and the subsequent buildup of the seasonal thermocline have important acoustic ramifications. For example, when the mixed layer transitions from the characteristic wintertime depth of approximately 100 m to the characteristic summertime depth of about 30 m, the low-frequency cutoff in the surface duct increases from roughly 180 Hz to about 1,100 Hz.

Finally we note that, particularly in the winter, thermal anomalies (i.e., deviations from climatology) of several degrees can form over vast expanses of the

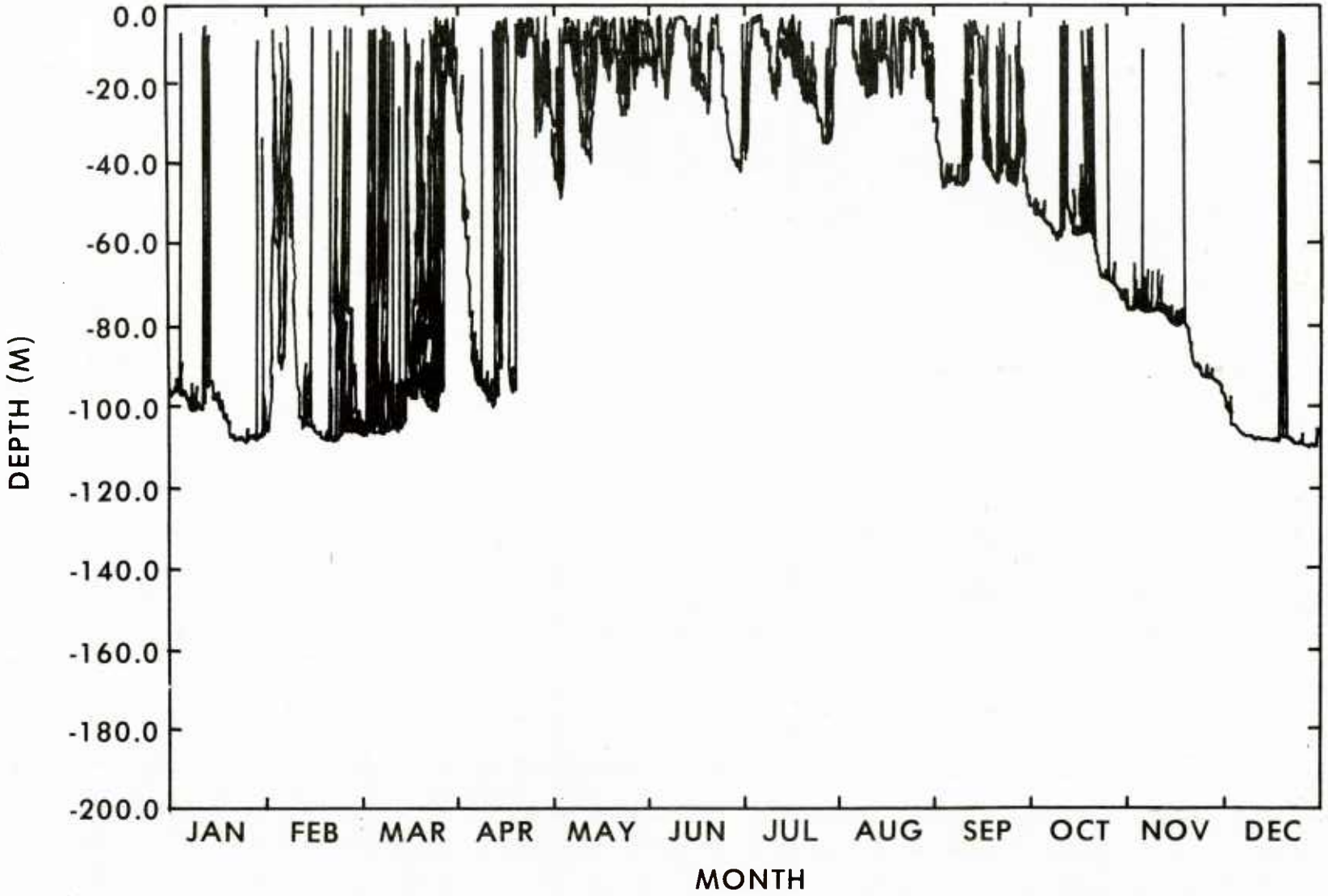

Figure 4. Predicted mixed-layer depth at Ocean Station November for 1961. The prediction was performed with the Mellor-Durbin Model and the mixed-layer depth was taken to be the shallowest level at which the temperature differed from the sea surface temperature by more than 0.1°C. Note the spring transition of the mixed-layer near the middle of April.

upper ocean and persist for months (see Haney, 1980; Kirwan et al., 1978). Using a forecast of adjustment toward climatology to generate the first-guess field in an objective analysis system will hinder analysis of thermal fields in these situations, especially during the formative stages of the anomalies.

A large portion of the upper ocean's nonclimatological response on time scales ranging from diurnal to seasonal is a direct result of anomalous vertical fluxes and/or anomalous Ekman currents (see Haney, 1980). Since synoptic mixed-layer models are well-suited to handling these phenomena, a major part of this nonclimatological evolution should be accountable with TOPS. Thus, TOPS can be used to improve ocean thermal analysis capabilities by supplementing an analysis scheme.

One way to accomplish this would be, in general terms, to initialize the model each day from an analysis, perform a forecast, and then feed the resulting 24-hour forecast thermal field back into the analysis as a first-guess field for the following day's analysis, in much the same way as is done in operational atmospheric forecast models (e.g., Bergman, 1979). This will tend to make the analysis dynamically consistent with the atmospheric forcing of the ocean, which should improve the reliability of the analyzed fields. This improvement should be particularly large in data-sparse regions, where the analyzed thermal field would no longer be constrained to stay very near the climatological state during the long periods between observations. Instead, the analysis on any particular day in these regions during these periods would be given essentially by the model-predicted first-guess field for that day. Thus, in effect, the model would be used to "fill in" the analysis in those regions of space and time where measured data is lacking. When observations do become available in a data-sparse region, the analysis would respond to them appropriately, with the net result that the model forecast would be updated with the new information. This approach is philosophically similar to that adopted by McPherson et al. (1979) in the design of the NMC Operational Global Atmospheric Data Assimilation System.

B. USE OF TOPS AS A REAL-TIME FORECAST SYSTEM

TOPS can routinely produce real-time, three-day forecasts of changes in the thermal structure of the upper ocean. Of course, if skillful atmospheric prediction capabilities are achieved on longer time scales (e.g., 5-10 days), then the TOPS forecast period will likewise be extended. In any event, the changes predicted by TOPS could prove to be tactically significant in some situations. For the purpose

of this discussion, these changes can be broadly grouped into two categories, (1) diurnal changes due to solar heating, and (2) longer-lasting changes due to the passage of atmospheric disturbances.

Midday solar heating of the upper ocean, especially under conditions of light winds and clear skies, tends to shallow the mixed-layer and increase its stratification. When the stratification in the upper layer becomes greater than about 0.01 $^{o}C\ m^{-1}$, the surface acoustic duct is destroyed. This produces the "afternoon effect" (see Urick, 1975) which is important in some acoustic surveillance applications and, in fact, played a critical role in many World War II ASW operations. Figure 5 illustrates the afternoon effect by showing time-depth contours of sound speed obtained by Shonting (1964) for typical diurnal variability in the tropics. Generally speaking, the afternoon effect is almost always large in the tropics but only appreciable in the mid- and high-latitudes under appropriate conditions in the summer and late spring.

The diurnal response of the upper ocean is obviously not resolved by the daily FNOC ocean thermal analysis. It is also obvious that generating the analysis more often would not help, since the problem is that the available data base is simply incapable of resolving the synoptic distribution of the mixed layer's diurnal response. This response is highly predictable with a synoptic mixed-layer model, however, especially since the phase of the solar heating is known exactly from purely geometrical considerations. To illustrate, we consider Figure 6, which shows the temperature at 6 m depth observed by the R. V. Discoverer during the BOMEX Experiment and a prediction of this temperature with the Mellor-Durbin model. The agreement is good, particularly with respect to phase. Similarly, Figure 7 shows observed and predicted temperature profiles at Discoverer for 1400 Local Time composited over the 6 days shown in the prior figure. As can be seen, the afternoon stratification of the mixed layer is well-represented by the Mellor-Durbin model. Thus, TOPS can be used to "fill in" the diurnal evolution of upper ocean thermal structure between synoptic analysis times and project this evolution several days into the future.

Furthermore, if strong solar heating is accompanied by several days of weak winds, then a warm shallow layer that persists over more than one diurnal cycle will form. Of course, if the mixed layer is very deep initially, the formation of this layer may result in the spring transition phenomenon illustrated by Figure 4. In any case, the point is that warming and shallowing of the mixed layer due to the

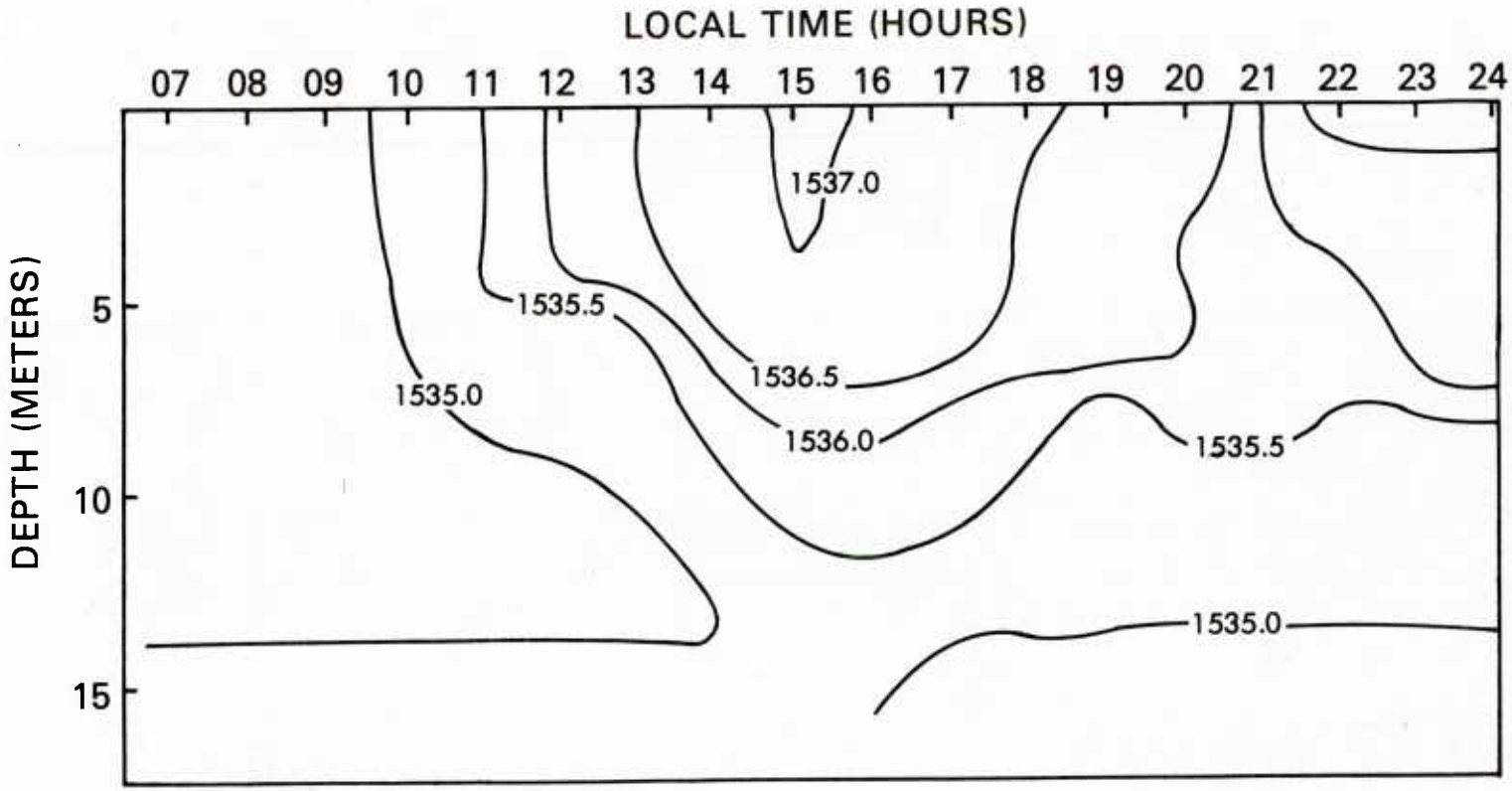

Figure 5. Time-depth contours of sound speed (ms^{-1}) in the upper ocean for typically observed diurnal evolution of the vertical temperature profile in the tropics (after Shonting, 1964).

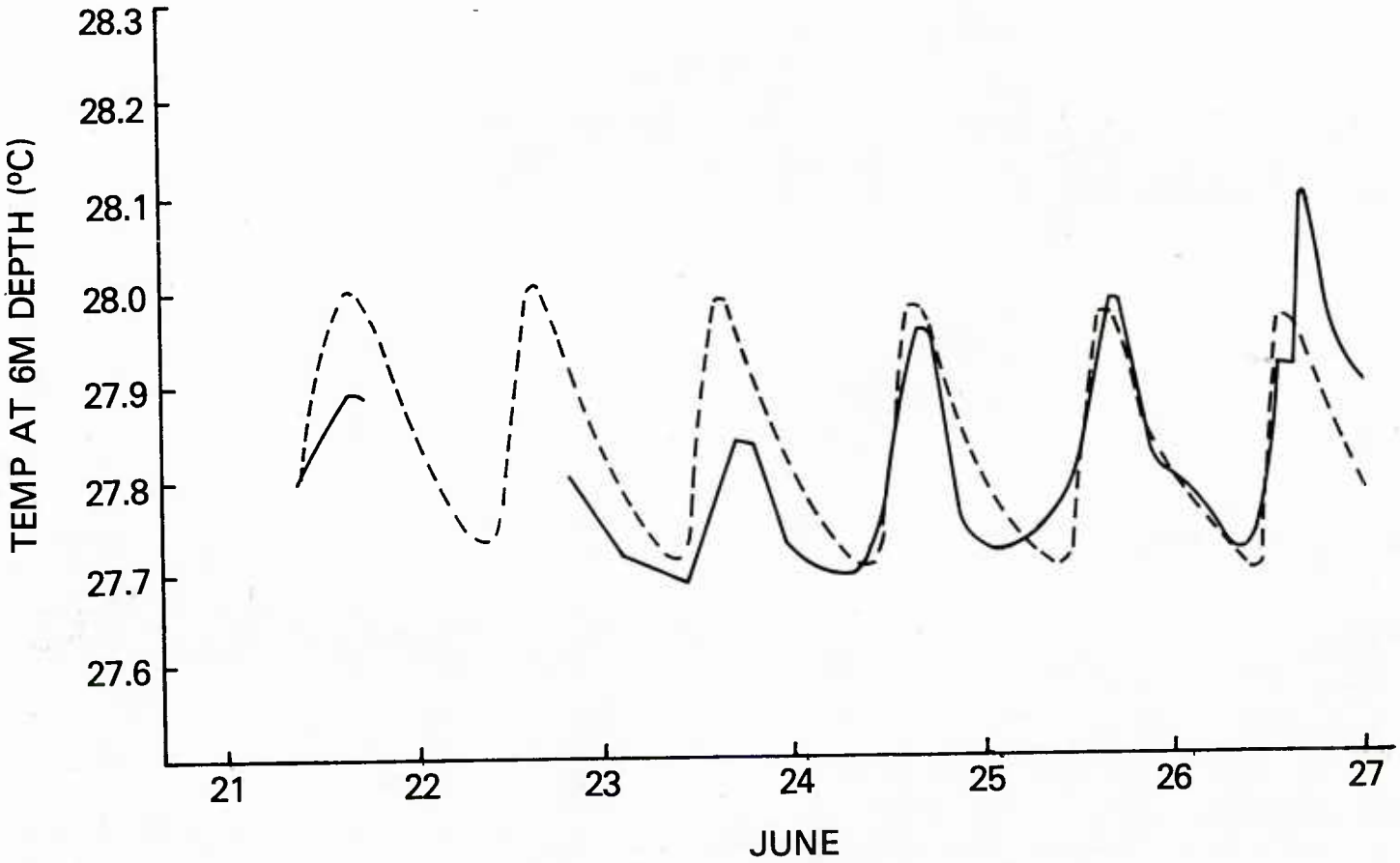

Figure 6. Time series of predicted (dashed line) and observed (solid line) temperatures at 6m depth at R.V. Discoverer during the BOMEX Experiment. The prediction was made with the Mellor-Durbin Model.

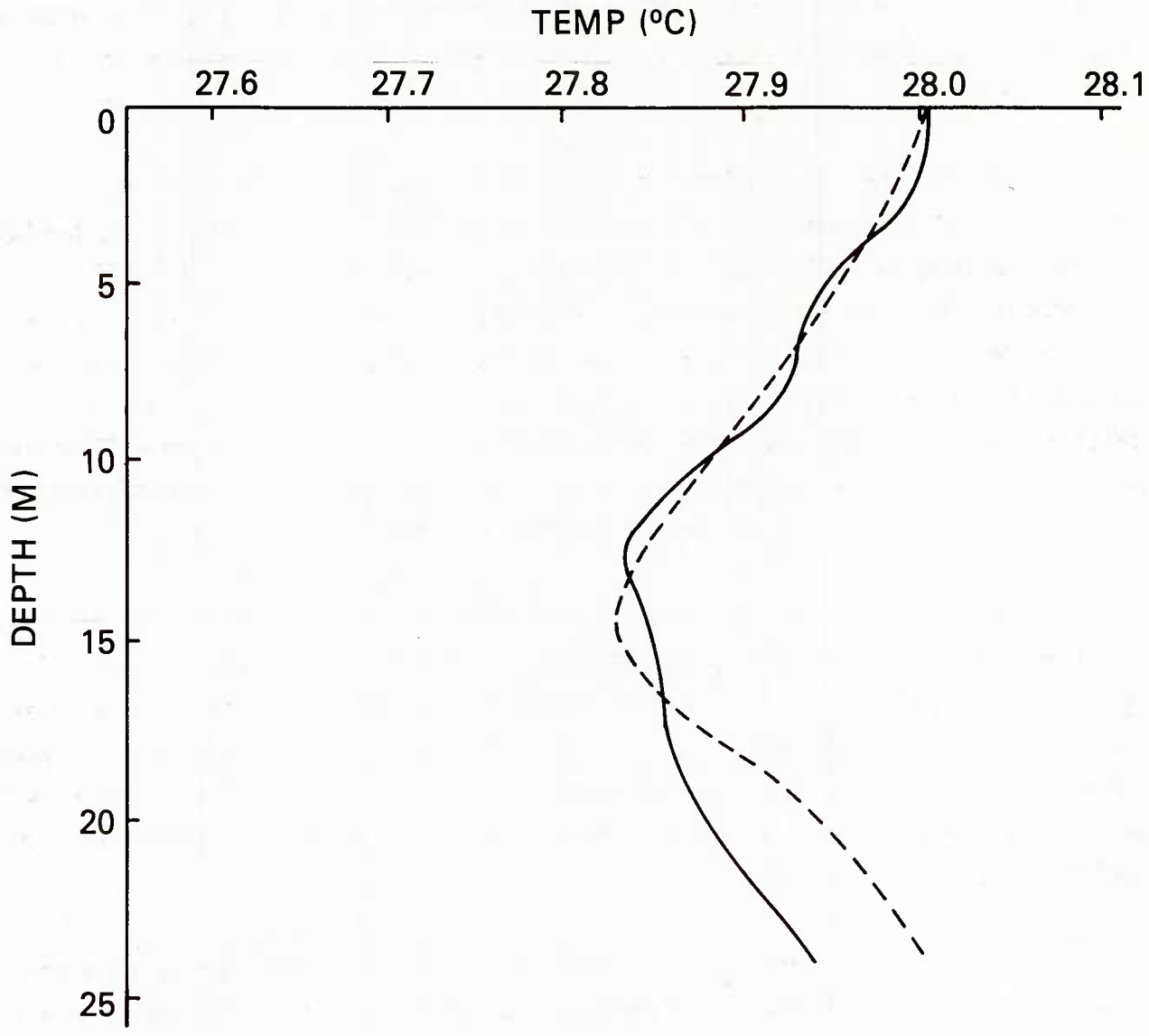

Figure 7. Predicted (dashed line) and observed (solid line) vertical temperature profiles at R.V. Discoverer composited for 1400 Local Time over the six days shown in Figure 6. The prediction was made with the Mellor-Durbin Model. Note that the temperature inversion below 15m depth was dynamically maintained by the salinity field.

passage of atmospheric high pressure systems, and the subsequent destruction of these warm shallow layers during periods of increasing winds, are predictable and can result in significant changes in ocean thermal structure over periods of a few days.

To illustrate, we consider Figure 8 which shows predictions by the Mellor-Durbin Model and observations from the MILE Experiment, which was conducted near Ocean Station PAPA (50°N, 145°W) during the summer of 1977. On Day 15 of the experiment, the temperature was isothermal to a depth of about 30 m (Figure 8(a)). By Day 18, following several days of weak winds, a warm shallow mixed layer of less than 5 m depth has formed (Figure 8(b)). Finally, on Day 22, the temperature has become isothermal to about 25 m depth in response to increasing winds. Note that the variability in the observations below the base of the mixed layer evident in Figure 8 is probably caused by internal waves.

An example of the response of the upper ocean on the three-day time scale to an atmospheric low-pressure system is given in Figure 9. This figure, from Price et al. (1978), shows the observed and predicted sea surface temperature at a location in the Gulf of Mexico during and after the passage of a cold front. A change of more than 1 C in 48 hours was observed and this is typical of what can occur when an intense synoptic weather disturbance passes over a relatively shallow mixed layer.

Another case of short time scale upper-ocean response to strong atmospheric forcing is given by Figure 10. This Figure shows the observed sea surface temperature at NOAA Data Buoy EB-10 during the passage of Hurricane Eloise and a prediction of this quantity with the Mellor-Durbin model. The eye of the storm passed directly over the buoy early on the 23rd. The sea surface temperature dropped 1.5 C in 24 hours and this change was well predicted by the model. Note that the major source of discrepancy between observation and prediction in Figure 10 is the lack of horizontal advection in the model (see Price, 1981).

Finally, in Figure 11 we see the temperature profile at a point in the Central North Pacific resulting from a three-day TOPS forecast that was performed in real time (see Clancy and Martin, 1981). Also shown are the initial and verifying temperature profiles at this point obtained from the EOTS analyses valid at the beginning and end of the forecast. An atmospheric cold front passed over the point in question during this period and, as can be seen from the figure, the strong

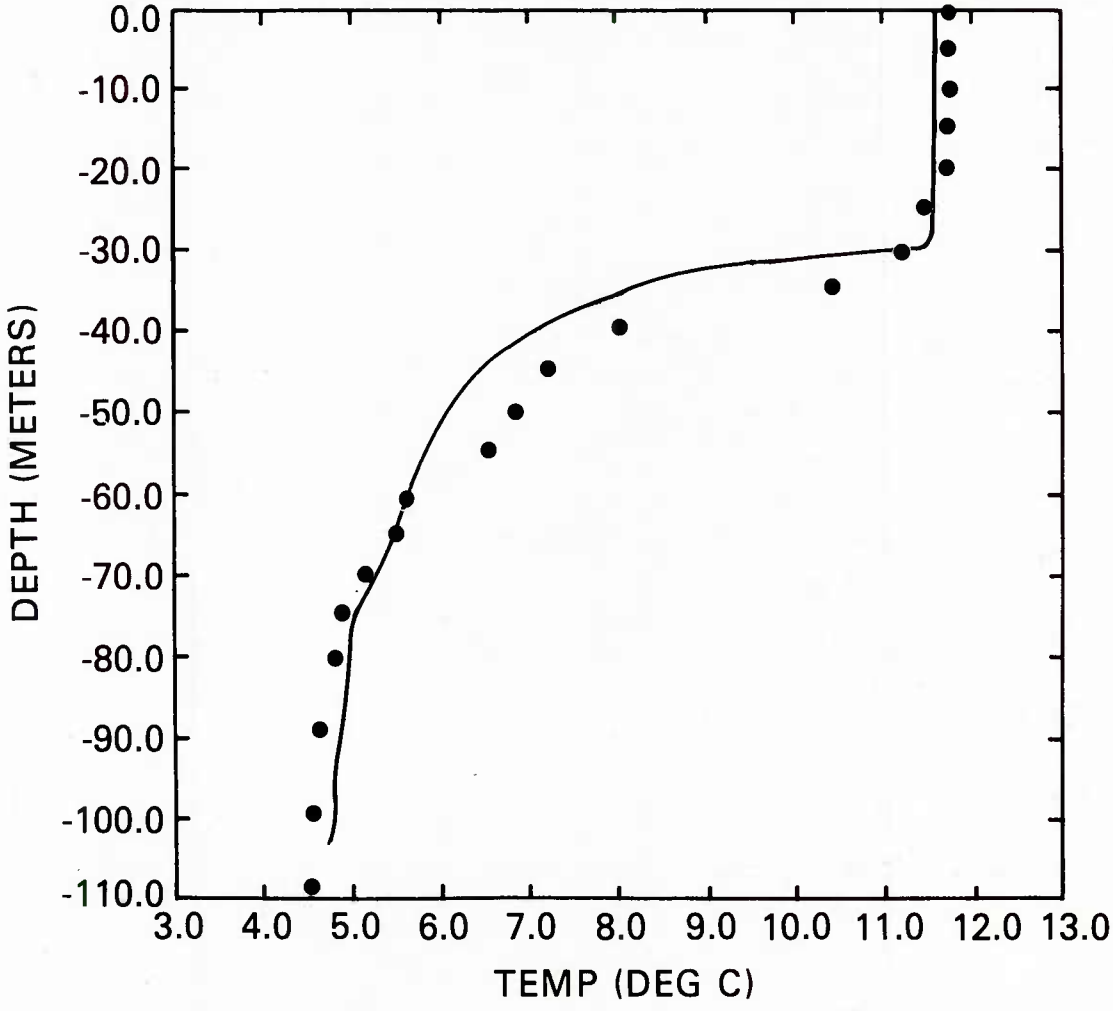

Figure 8(a). Vertical temperature profile predicted with the Mellor-Durbin Model (solid line) and observations at 0715 Local Time on Day 15 of the MILE Experiment.

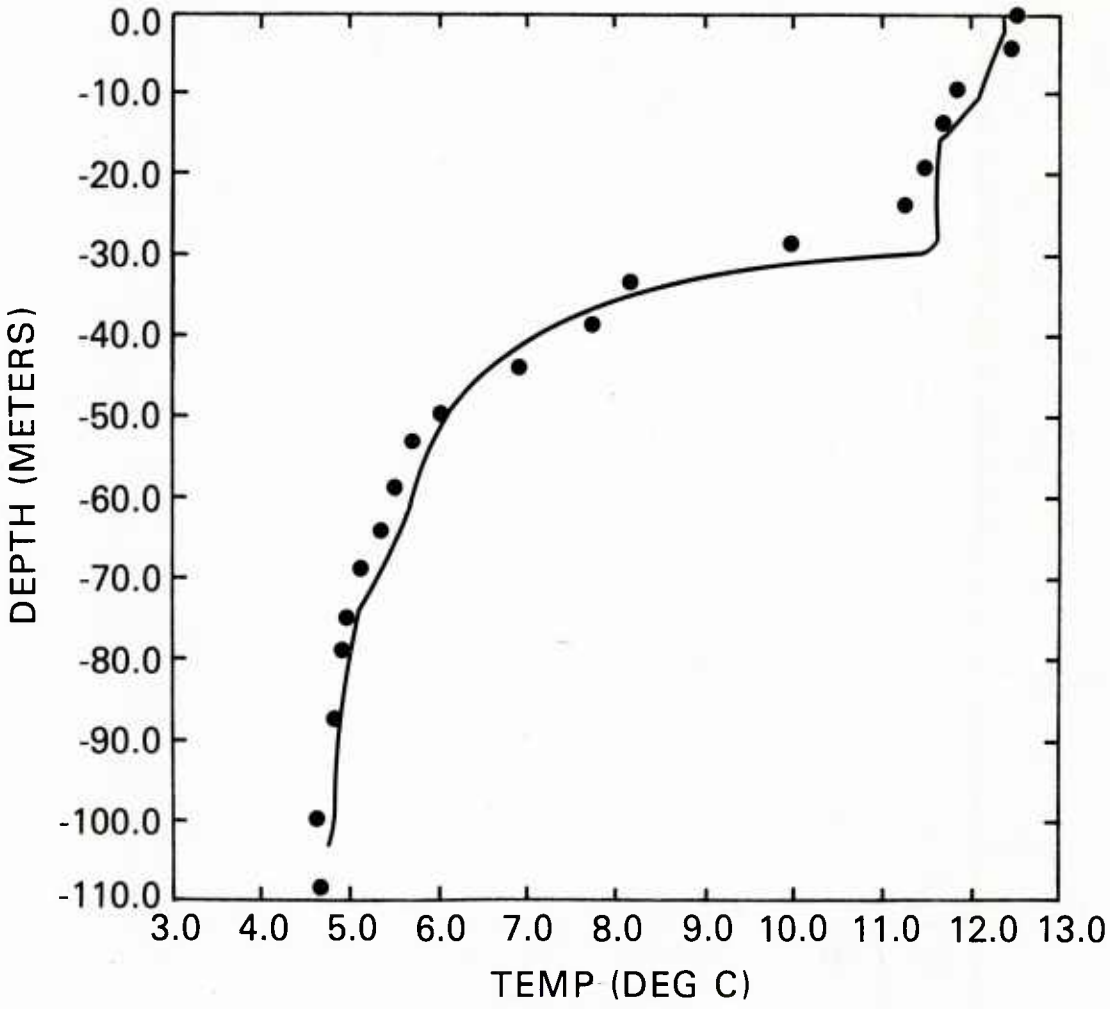

Figure 8(b). Same as 8(a) but for 1245 Local Time on Day 18.

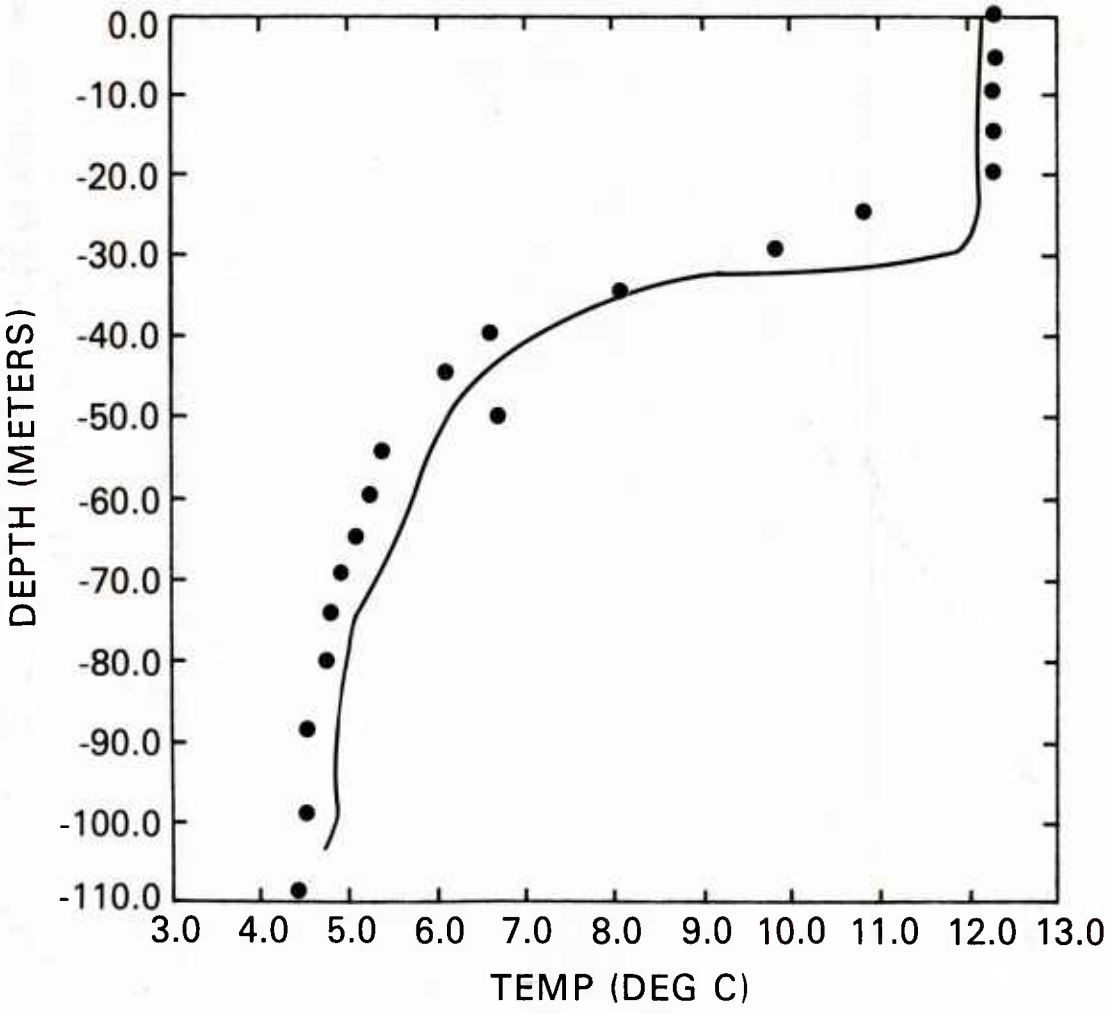

Figure 8(c). Same as 8(a) but for 1024 Local Time on Day 22.

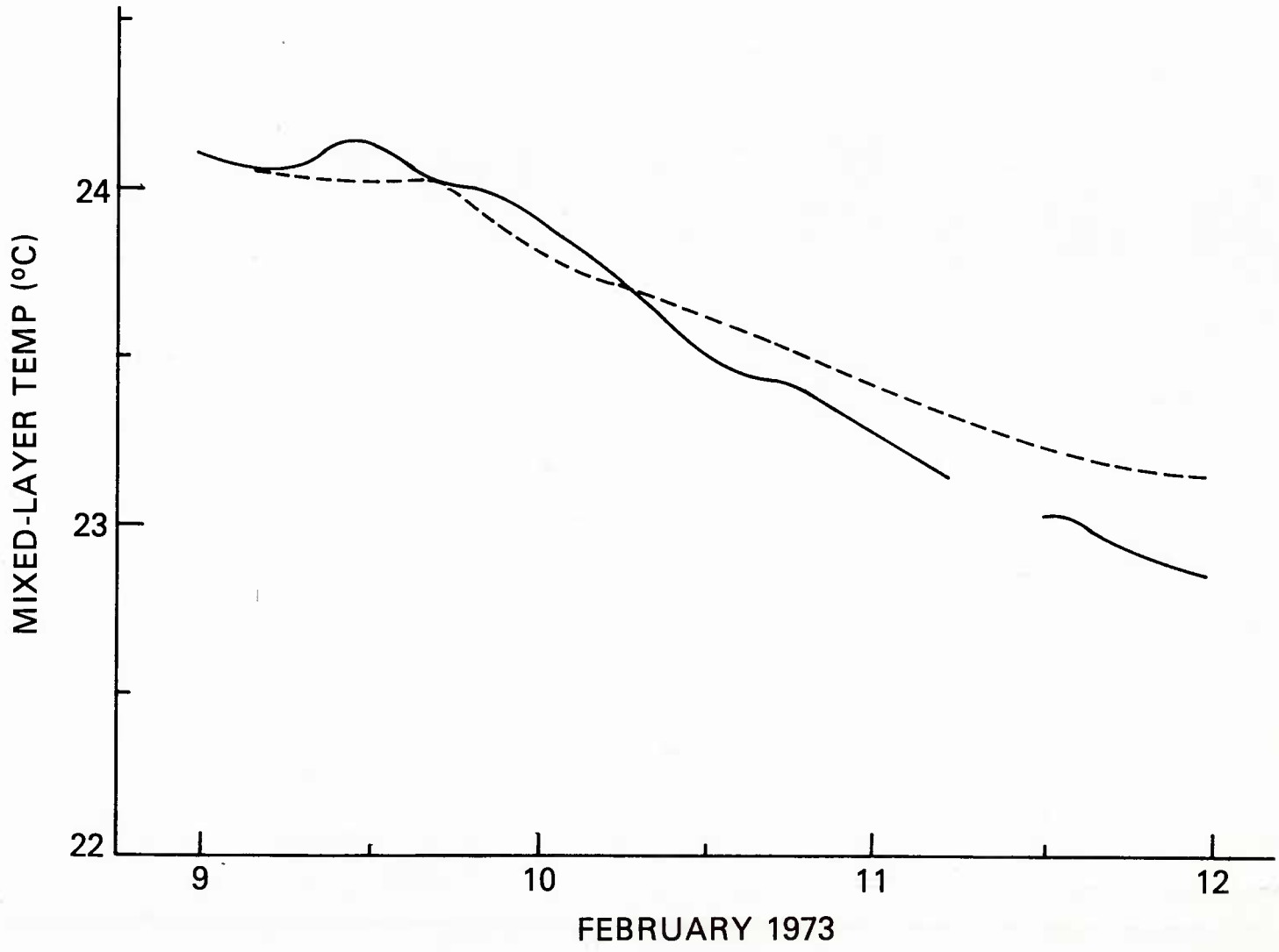

Figure 9. Predicted (dashed line) and observed (solid line) mixed-layer temperature response to the passage of an atmospheric cold front in the Gulf of Mexico (after Price et al., 1978).

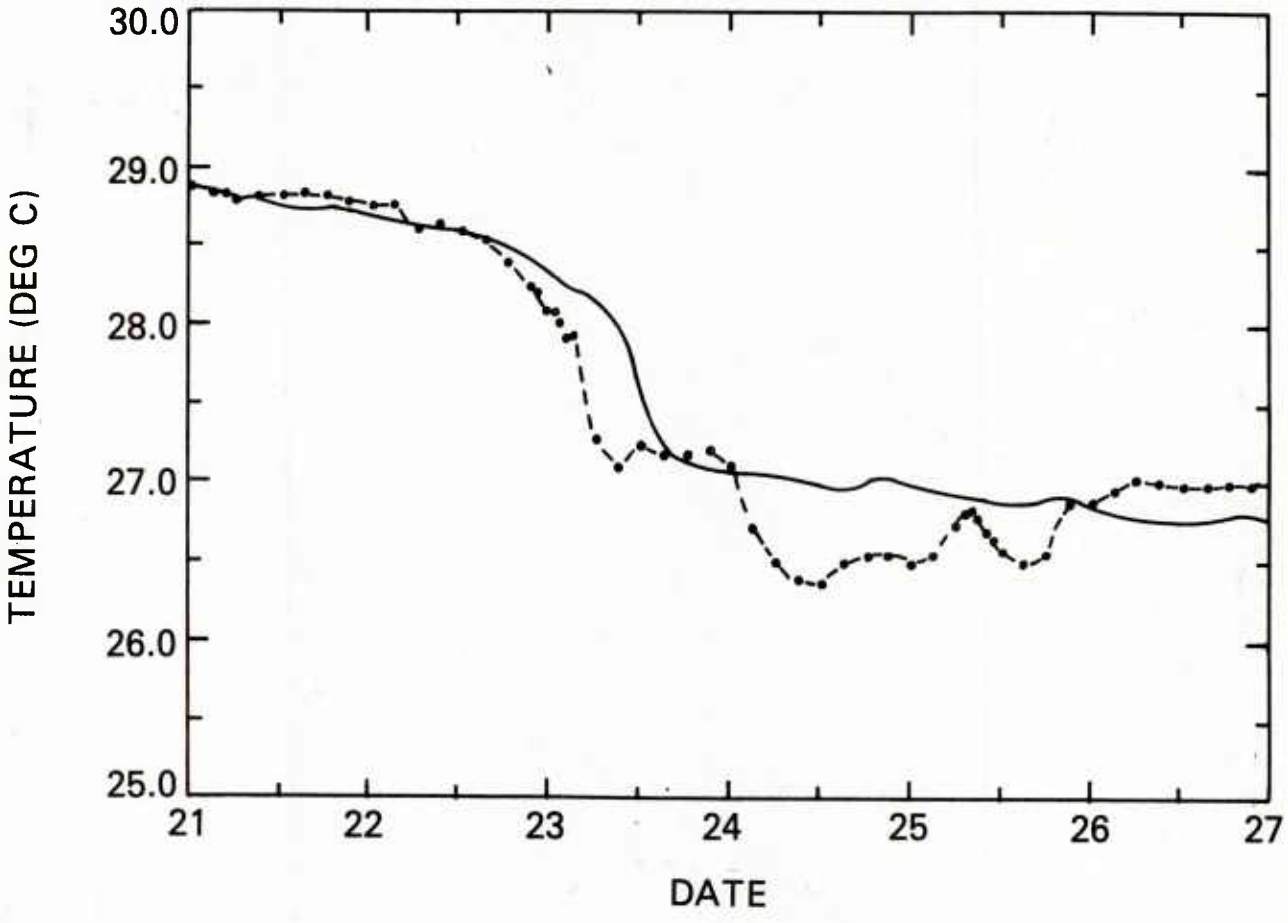

Figure 10. Predicted (solid line) and observed (dashed line) sea surface temperature response to the passage of Hurricane Eloise over NOAA data buoy EB-10. The prediction was made with the Mellor-Durbin Model.

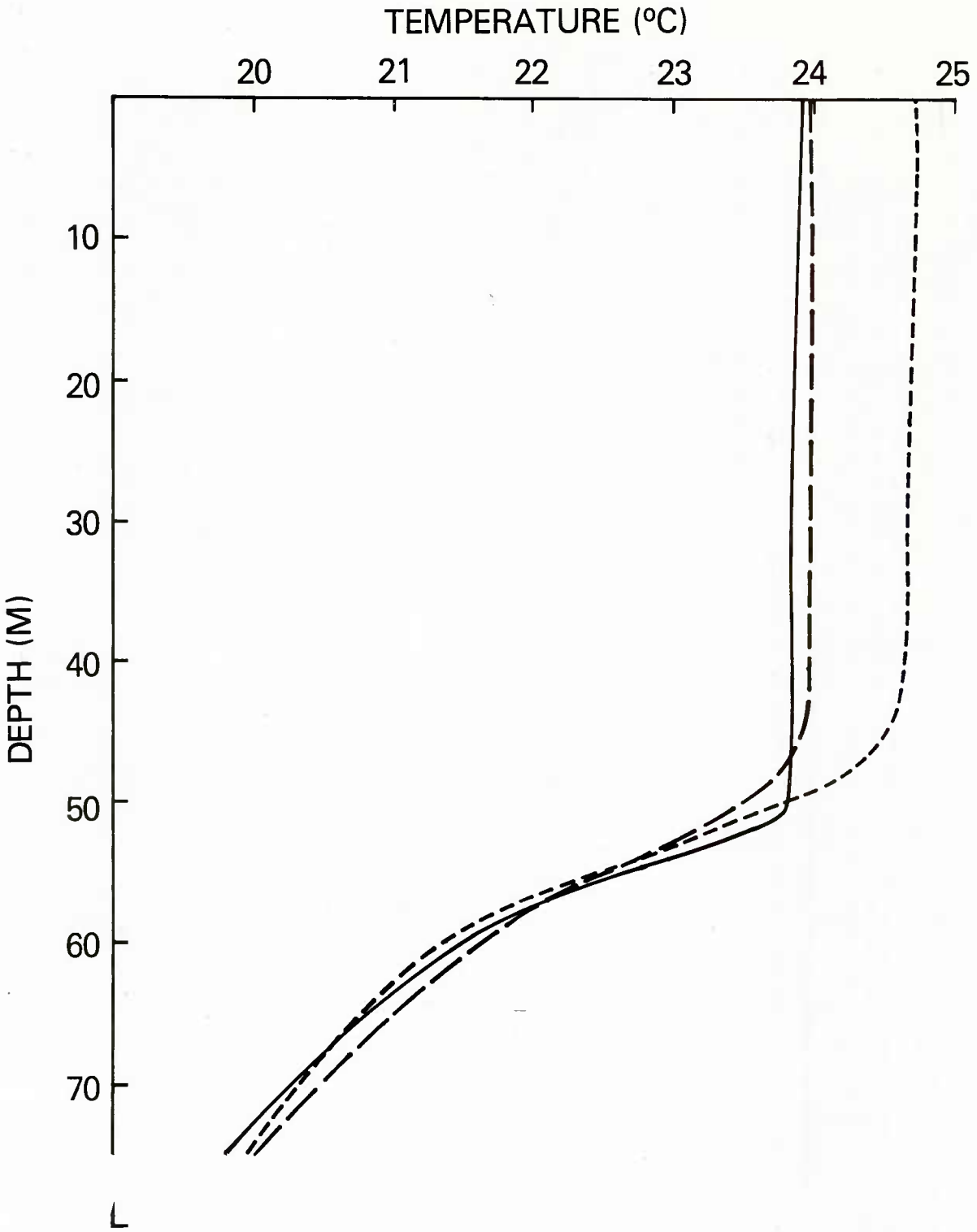

Figure 11. Initial (dashed line), predicted (bar line), and verifying (solid line) vertical temperature profiles at 29.4°N, 179.5°W for a three-day TOPS forecast from 0Z 5 November 1979.

cooling associated with it made persistence (as well as adjustment toward climatology) a poor forecast compared to that of the model.

The capability to forecast the types of upper ocean developments discussed in this section several days in advance could prove useful in planning the deployment of ASW sensors and platforms and the optimum acoustic routing of Carrier Task Groups (Dunlap and Tierney, 1981). Joint acoustic/environmental modeling studies are currently underway at NORDA in an effort to achieve a more quantitative assessment of the impact of this forecast capability on the Navy's acoustic products.

C. USE OF TOPS TO PROVIDE CURRENT VELOCITY INFORMATION

The synoptic mixed-layer models implemented via TOPS represent the Ekman plus inertial component of the current. As mentioned previously, Ekman advection can play a major role in the formation of large-scale ocean thermal anomalies. The omnipresent inertial oscillations, however, are no less important to naval concerns.

As demonstrated first by Pollard and Millard (1970), inertial oscillations in the mixed layer are highly predictable with the type of simple physics included in TOPS. This is because they are essentially locally forced phenomena whose characteristics at any given time depend primarily on the latitude and the history of the local surface wind stress over the previous 10-15 day period. Changes in the surface wind stress tend to excite inertial oscillations, especially if the stress vector rotates clockwise in the Northern Hemisphere with an angular velocity close to that of inertial. This resonance phenomenon can rapidly generate inertial oscillations with amplitudes in excess of 1 kt (Pollard and Millard, 1970) and produce asymmetric mixed-layer deepening (due to mean-flow-shear turbulence generation) between either side of an advancing storm track (Price, 1981).

An example of the predictability of inertial oscillations is afforded by Figure 12, which shows the observed current at a depth of 50 m below NOAA Data Buoy EB-10 during the passage of Hurricane Eloise and a prediction with the Mellor-Durbin Model. The mixed layer deepened from 32 to 52 m in response to the approaching storm and this caused the inertial oscillations evident in the record beginning on the 23rd. As can be seen, both the amplitude and phase of these oscillations are well-represented by the model.

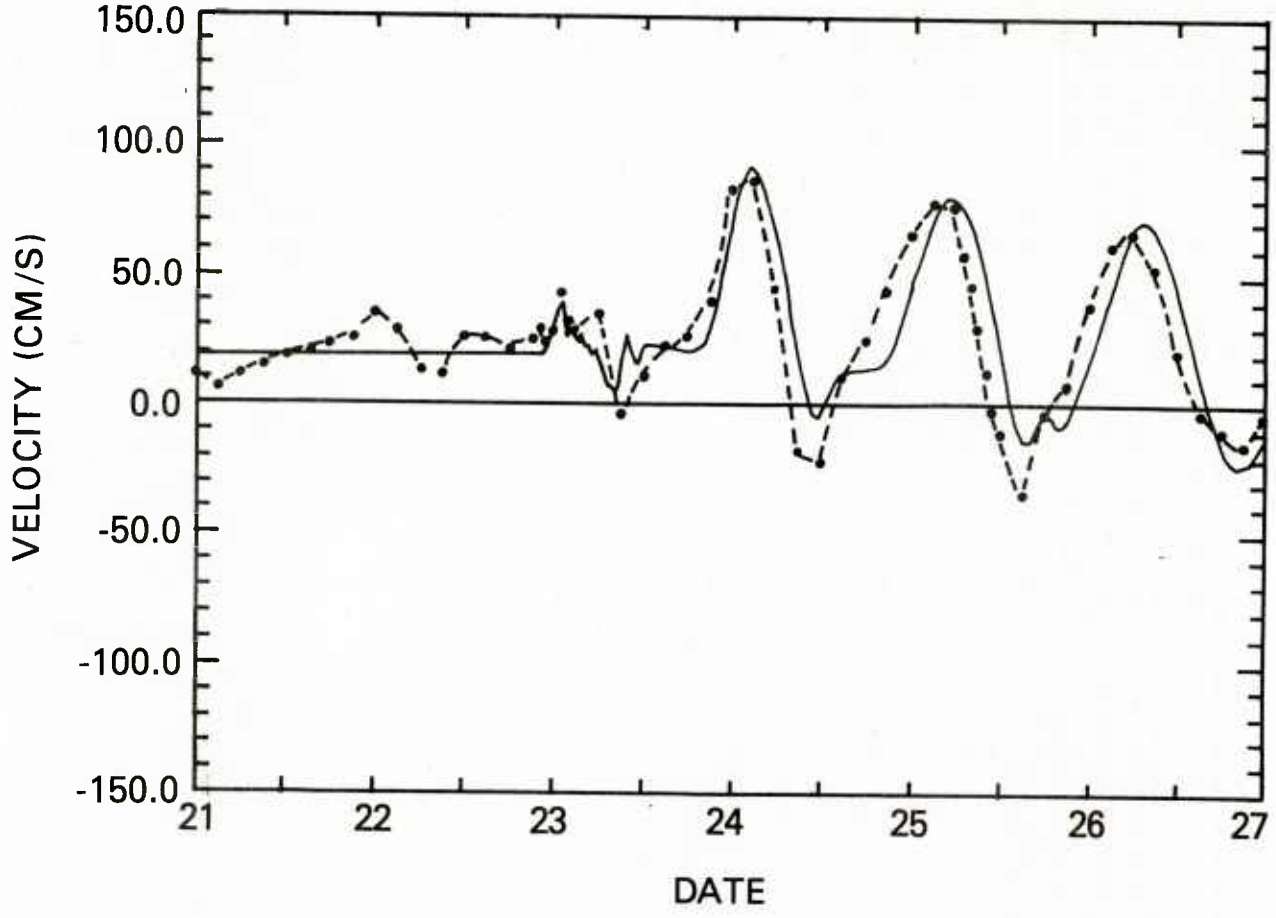

Figure 12. Predicted (solid line) and observed (dashed line) NS component of the current at 50m depth at NOAA data buoy EB-10 during the passage of Hurricane Eloise.

There is a substantial amount of useful information in the current velocity fields predicted by TOPS. This is particularly true during the period following 10-15 days after a "cold start" of the model (see Section II. D) since, from this point on, the current field becomes independent of the cold-start initial conditions and dependent primarily upon the integrated effect of the wind stress over the previous 1-2 week period. Thus, the model keeps track of the amplitude and phase of the inertial oscillations as well as the magnitude and direction of the Ekman drift, and makes this information available on a real-time synoptic basis. This would be of use in search and rescue operations and perhaps navigation.

Knowledge of the vertical current shear in the mixed layer and near its base is also useful to the Navy since it is important in certain non-acoustic ASW applications. This shear is primarily due to the component of the current represented in TOPS which, consequently, can be used to provide its real-time synoptic distribution. Experience with TOPS has shown that the shear field exhibits considerable variability in both time and space as inertial currents and mixed-layer depths respond to passing storms. Furthermore, as shown by Warn-Varnas and Dawson (1981), rather complicated vertical current profiles can result when the wind stress and mixed-layer depth change rapidly with time.

IV. TEST AND EVALUATION OF TOPS

A. BACKGROUND

The turbulence parameterization model currently implemented in TOPS, and similar models, have been tested favorably in a number of one-dimensional studies (e.g., Mellor and Yamada, 1974; Mellor and Durbin, 1975; Martin, 1976; Thompson, 1976; Price et al., 1978; Clancy, 1979; Warn-Varnas and Piacsek, 1979; Yamada, 1979; Warn-Varnas et al., 1981; Martin, 1981; Martin and Thompson, 1981). Although far from perfect, these models have proved capable of predicting a significant portion of oceanic mixed-layer variability. Examples of this capability have been given in prior sections, and yet another case is shown in Figure 13.

This figure shows time series of wind speed, sea surface temperature, and mixed-layer depth observed at Ocean Station November during June 1961, along with a prediction by the Mellor-Durbin Model, which is currently used in TOPS. The model prediction was initiated on 1 January 1961 and forced with the standard meteorological parameters observed at the ocean station. A simplified treatment of horizontal

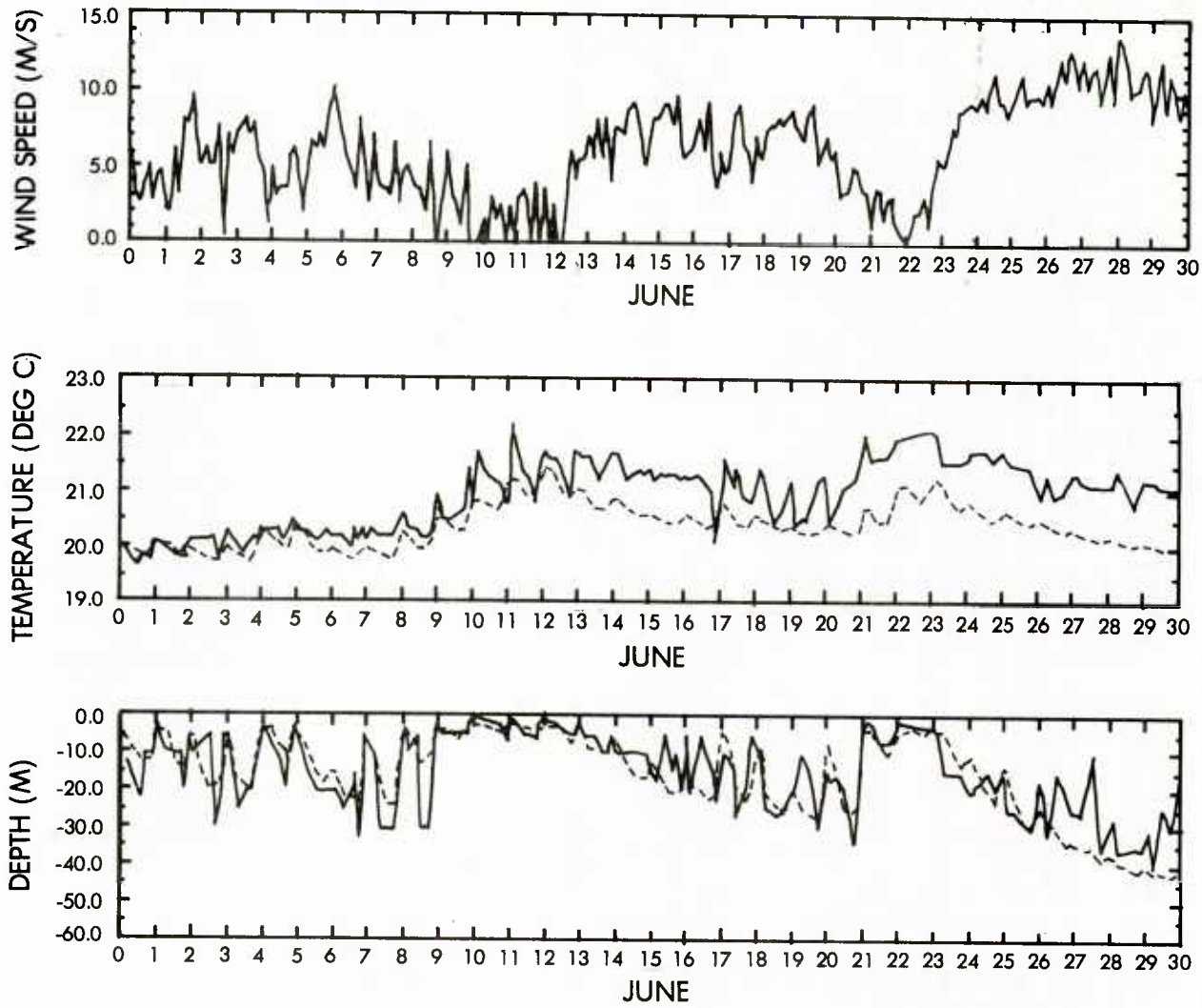

Figure 13. Observations and predictions at Ocean Station November during June of 1961. *Upper panel*: observed wind speed. *Middle panel:* observed (solid line) and predicted (dashed line) sea surface temperature. *Bottom panel*: observed (solid line) and predicted (dashed line) mixed-layer depth. The predictions were made with the Mellor-Durbin Model.

advection was included by advecting the climatological temperature field with the instantaneous current obtained from the model. At the beginning of June, even after six months of integration, both the sea surface temperature and mixed-layer depth verify well against the observations. Although the sea surface temperature drops about 1 C below the observations on the 14th (probably due to an advective effect), both sea surface temperature and mixed-layer depth tend to parallel the major trends throughout the record. Specifically, the warming/shallowing events of June 9-12 and 21-23 are well-predicted by the model as are the deepening/cooling trends of June 13-20 and 24-30. The correlation of these developments with the wind speed, of course, is high, as can be seen from the figure.

Results from one-dimensional studies using data from ocean weather stations, buoys, or special field experiments, such as shown in Figure 13 and earlier examples, increase our confidence in mixed-layer models and lead us to think that a forecast system such as TOPS can be successful. In the evaluation of TOPS, however, the key issue is synoptic verification over vast areas rather than one-dimensional verification at a few isolated locations. In addition, verification of TOPS forecasts is, to a great extent, a test of the FNOC operational data base which supplies the ocean model with its initial conditions, upper boundary conditions, and verification fields.

The maximum period over which the thermal fields can be forecast in real time with TOPS is tied to the predictive capabilities of atmospheric models and is currently limited to three days. Thus, verification of TOPS forecasts on the three-day time scale is relevant and important. Verification over longer time scales is also important; when the model is used to generate first-guess fields for the ocean thermal analysis system that provides its initial conditions, the model integration could be carried along for months in a data-sparse region before being updated with observations.

In this paper we will address verification of TOPS only on the three-day time scale by considering forecasts with the non-advective model. Verification over longer time scales with the advective model will be the topic of future studies.

In performing short time scale synoptic verification of large-scale ocean thermal forecasts such as we undertake here, one is confronted with several facts. First of all, the verification temperature fields must be obtained from an objective

analysis scheme since observations will never be available precisely at the grid-points of the model. Furthermore, the same analysis scheme that provides the initial conditions for the forecast must be used to generate the verification fields. This is because, as shown by Barnett et al. (1980), different analysis schemes can produce fields from the same data input that differ by a large amount. If different analysis schemes are used to supply the initial and verification fields, apparent changes due purely to inherent differences between the schemes could mask any real changes in the thermal field that may have occurred during the forecast period. Therefore, since TOPS is initialized from the EOTS analysis scheme it must also be verified with fields from that analysis scheme.

Because of the paucity of XBT observations reported daily to FNOC, synoptic changes in the subsurface thermal field on the time and space scales of interest here are inadequately resolved by the EOTS analysis. Changes in the sea surface temperature field, however, are marginally resolved on these scales since the number of surface ship observations assimilated into the daily analysis is about one order of magnitude greater than the number of XBT observations available. Consequently, our approach has been to focus generally on sea surface temperature for short time scale synoptic verification of TOPS. Note that the sea surface temperature field is particularly important to the Navy because it is used in at least twelve operational FNOC products. In addition, given the depth of a water column, the existence of shallow acoustic convergence zones due to refraction of ray paths in the deep sound channel depends critically on the sea surface temperature.

The surface ship observations reported routinely to FNOC are a roughly equal mix of engine intake and bucket temperature measurements and are made available in real time via the WMO-sponsored Integrated Global Ocean Station System (IGOSS) Program (WMO Report 466). The standard error of these observations is generally comparable to the synoptic-scale changes in sea surface temperature that typically occur over a period of a few days. Therefore, verification results must be interpreted carefully since real synoptic-scale changes in sea surface temperature (signal) could easily be masked by spurious analyzed changes (noise).

B. PATTERN-OF-CHANGE CORRELATION TECHNIQUE

The pattern-of-change correlation technique, which has proved valuable in verification of atmospheric models (see Dobryshman, 1972), is useful for short time scale synoptic verification of TOPS. This method is particularly well-suited for

verifying forecasts in which the typical model-predicted changes are only slightly larger than the noise level of the verifying analyses, which is the case here.

In this approach we calculate the pattern correlation between the forecast and analyzed changes in temperature R_{FA} from

$$R_{FA} = \frac{\overline{\Delta T_F' \Delta T_A'}}{\sigma_F \sigma_A} \tag{10}$$

where ΔT_F is the forecast temperature change obtained from the model, ΔT_A the analyzed temperature change over the same period obtained from EOTS, σ_F the standard deviation of the forecast temperature change, and σ_A the standard deviation of the analyzed temperature change. Here the overbar represents an average over all gridpoints in a selected region, and primes indicate departures from this average. A value of 1 for R_{FA} implies that the model predicts the pattern of the analyzed change perfectly while a value of 0 indicates that the model has no skill in predicting this pattern.

The significance of R_{FA} can be further explored by representing ΔT_F and ΔT_A as

$$\Delta T_F = \Delta T_T + \varepsilon_F \tag{11}$$

$$\Delta T_A = \Delta T_T + \varepsilon_A \tag{12}$$

where ΔT_T is the true temperature change, ε_F the error in the forecast temperature change, and ε_A the error in the analyzed temperature change. Note that ΔT_T, ε_F, and ε_A are all unknown quantities.

Now, the error in the analyzed temperature change is a result of factors that are unrelated to the model-predicted temperature change. Thus, we have

$$\overline{\Delta T_F' \varepsilon_A'} = 0 \tag{13}$$

Similarly, we expect no particular relationship between the error in the analyzed change and the error in the forecast change. Therefore,

$$\overline{\varepsilon'_F \varepsilon'_A} = 0 \tag{14}$$

which, along with (11) and (13), yields

$$\overline{\Delta T'_T \varepsilon'_A} = 0 \tag{15}$$

From (10), (12), and (13) we obtain

$$R_{FA} = \frac{\overline{\Delta T'_F \Delta T'_T}}{\sigma_F \sigma_A} \tag{16}$$

or

$$R_{FA} = \frac{\sigma_T}{\sigma_A} R_{FT} \tag{17}$$

where σ_T is the standard deviation of the true temperature change and R_{FT} is the pattern correlation between the forecast and true temperature changes. The coefficient R_{FT} is the quantity we are most interested in but, like σ_T, is unknown at this point.

From (12) and (15) we get

$$\sigma_A^2 = \sigma_T^2 + \sigma_{A\varepsilon}^2 \tag{18}$$

where $\sigma^2_{A\varepsilon}$ is the variance of the error in the analyzed change. This implies

$$\frac{\sigma_T}{\sigma_A} < 1 \tag{19}$$

which, from (17), shows that R_{FA} underestimates R_{FT}. Furthermore, if the analyzed change is dominated by noise, $\sigma_T/\sigma_A \ll 1$ and therefore $R_{FA} \approx 0$ even if R_{FT} is significantly different from zero. Thus, although $R_{FA} > 0$ implies that the model has skill in predicting the pattern of the true temperature change, $R_{FA} \approx 0$ does not necessarily imply that the model has no skill in predicting this pattern.

The ability of a model to predict the pattern of upper ocean thermal change, as reflected by R_{FT}, is an important indication of its usefulness. On the three-day time scale, this pattern of change is dictated essentially by the location and movement of synoptic scale weather disturbances. Positive values of R_{FT} indicate that the model can supply useful information on the synoptic response of the upper ocean to these disturbances. As discussed in Section III.A, this information can be used to advantage in ocean thermal analysis.

To illustrate use of the pattern-of-change correlation technique for short time scale verification of the non-advective TOPS model, we consider Figure 14. The three points linked by the dotted line in the figure are values of R_{FA} for the vertically averaged temperature between the surface and 75 m depth in a zonal band between 20 and 50°N for forecast times of 1, 2, and 3 days from 0Z 5 November. The error bars indicate 95% confidence limits. As can be seen from the figure, the forecast temperature change is correlated with the analyzed change at a higher than 95% level of confidence for all three forecast times. From the previous discussion, this indicates skill in the forecast. Note the monotonic downward trend in R_{FA} with increasing forecast time. This is probably a result of errors in the atmospheric forcing fields (forecast from 0Z 5 November by the FNOC PE and PBL models) growing with increasing forecast time.

The three points in Figure 14 linked by the solid line are values of R_{FA} for the same domain produced by a control experiment. In this experiment, exactly the same model, initial conditions, and verification fields present in the original case were used, but the atmospheric forcing fields were obtained from the

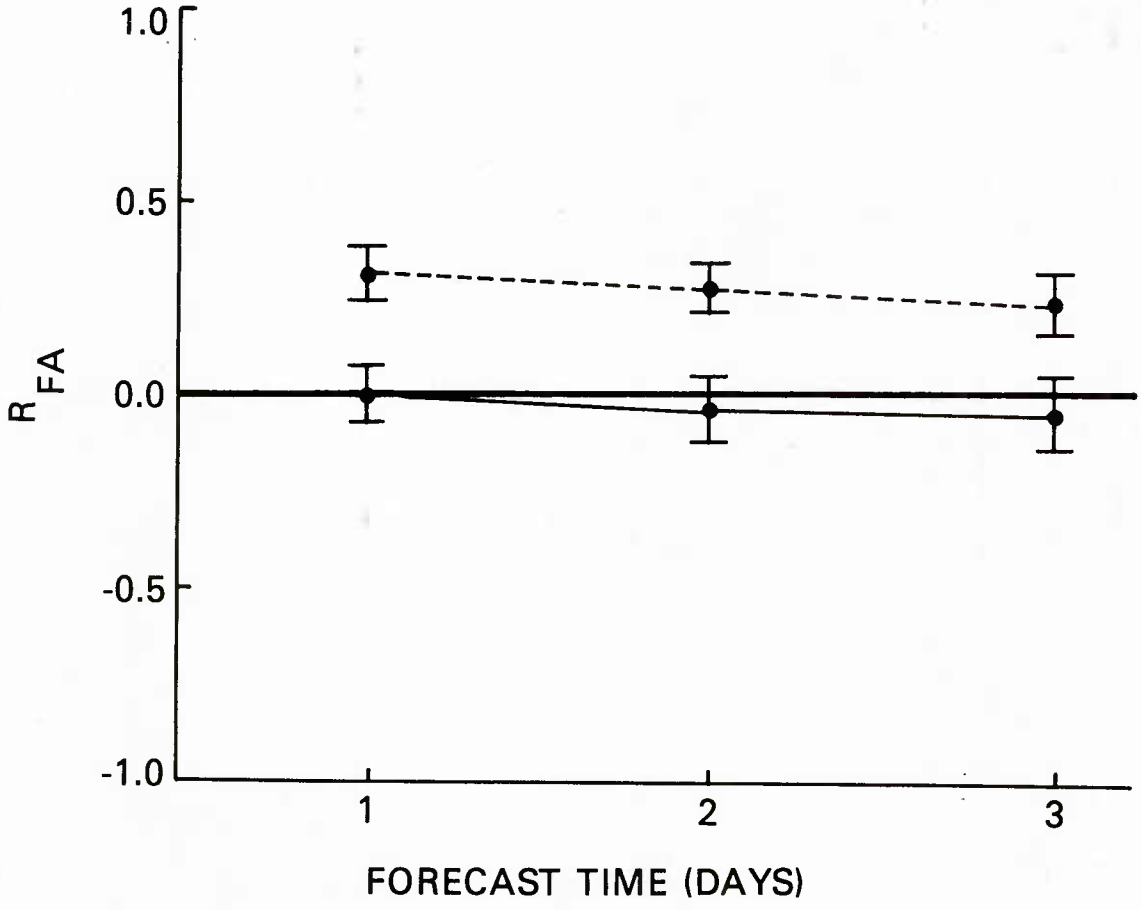

Figure 14. The points connected by the dashed line are pattern correlations between forecast and analyzed changes in the vertically averaged temperature in the upper 75m in a zonal band between 20° and 50°N for forecast times of one, two, and three days from 0Z 5 November 1979. The points connected by the solid line are pattern correlations between the same quantities resulting from a control experiment which differed from the original experiment only in that the surface fluxes which drove the forecast were obtained from a randomly selected three-day period in February. The error bars represent 95% confidence limits.

FNOC system for a randomly selected three-day period in February. The weather patterns for this period showed no particular relationship to those of the one beginning at OZ 5 November and, as expected, there is no indication of skill in the forecast as the correlations do not differ significantly from zero. This shows the importance of synoptic weather patterns in forcing three-day time scale changes in upper ocean thermal structure. It also illustrates the ability of EOTS to respond to these changes and demonstrates the ability of TOPS to predict these changes.

A further demonstration of this ability is afforded by the preliminary FNOC test and evaluation of TOPS. In this program, a sequence of thirty-seven daily, three-day forecasts was performed with the non-advective model using operational fields from the fall of 1980. The thermal field for each three-day forecast was initialized from the daily EOTS analysis and verified against the EOTS analysis valid at the end of each forecast period. Verification efforts focused primarily on sea surface temperature changes in two regions: the Pacific between 30-60°N and 115°W-130°E, and the Atlantic between 30-60°N and 0-80°W. Figure 15 shows a typical three-day distribution of surface ship observations in these areas.

The pattern correlation between the forecast and analyzed sea surface temperature changes for each three-day period R_{FA} is calculated and displayed in time series form in Figure 16. As seen from Figure 16(a), there is a consistent indication of forecast skill in the Pacific as this quantity is positive throughout the entire record. The average value of R_{FA} in this region during the 37-day period was 0.27.

As shown by Figure 16(b), R_{FA} for the Atlantic oscillates between near 0.0 and about 0.5 with a period of approximately one week. The average value during the experimental period was 0.25. The periodicity evident in this figure is probably related to synoptic-scale storm activity since it corresponds roughly to the life cycle time scale of low pressure systems moving across the Atlantic. The lack of this marked periodicity in the Pacific (see Figure 16(a)) may be due to the fact that our Pacific verification region is about twice as large as the Atlantic one, which implies that the statistics in this region are less influenced by an individual storm.

The results presented in Figure 16 are sufficient to establish that TOPS has skill on the three-day time scale. If the model had no skill, then the correlations shown in this figure would simply fluctuate with small amplitude about zero.

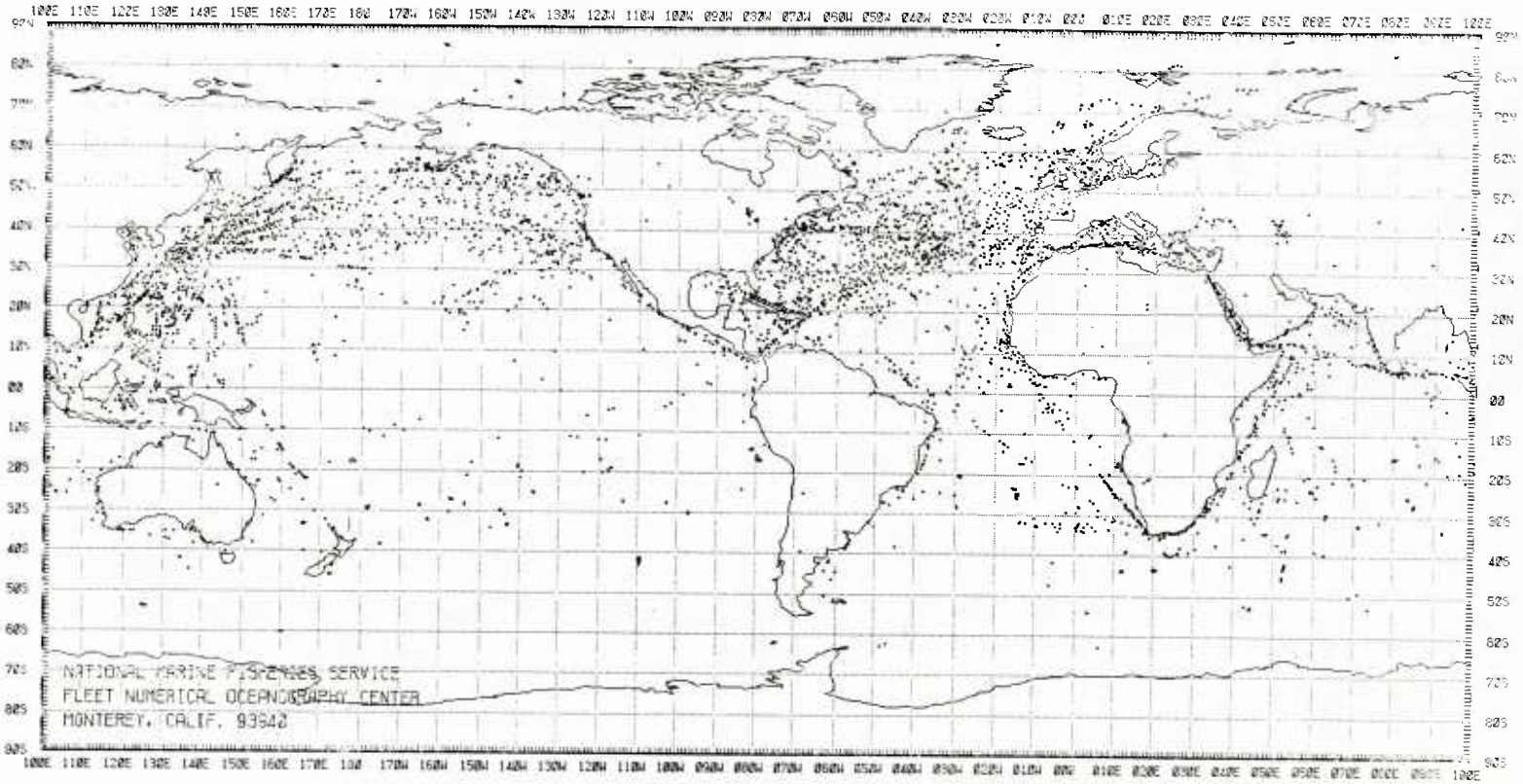

Figure 15. Typical three-day distribution of unclassified surface ship observations during the experimental period.

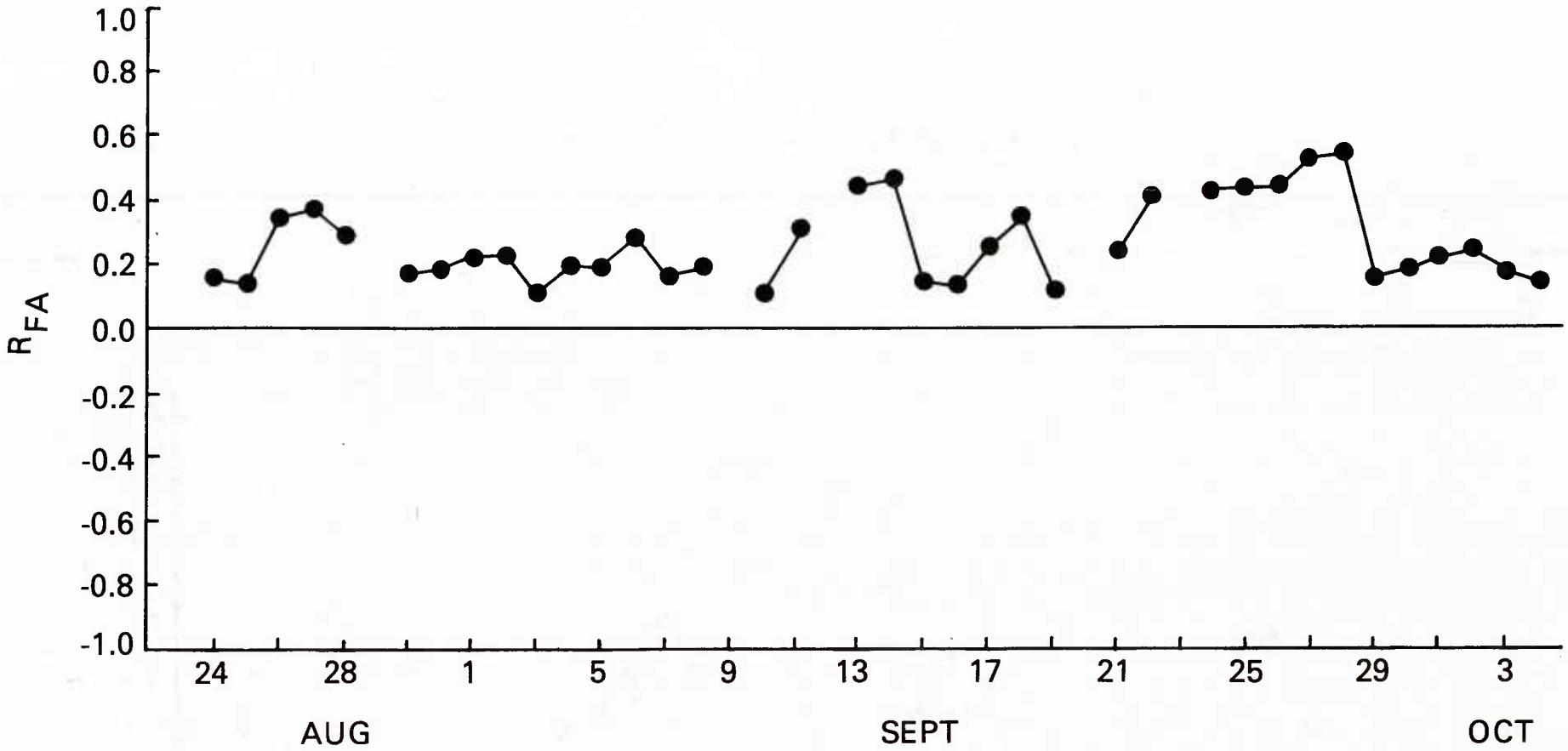

Figure 16(a). Pattern correlations between forecast and analyzed three-day changes in sea surface temperature in the North Pacific between 30° and 60°N, and 130°E and 115°W for a sequence of thirty-seven daily, three-day forecasts. Each correlation is plotted on the day corresponding to the beginning of the relevant forecast period and gaps indicate days on which missing data precluded the generation of model forecasts.

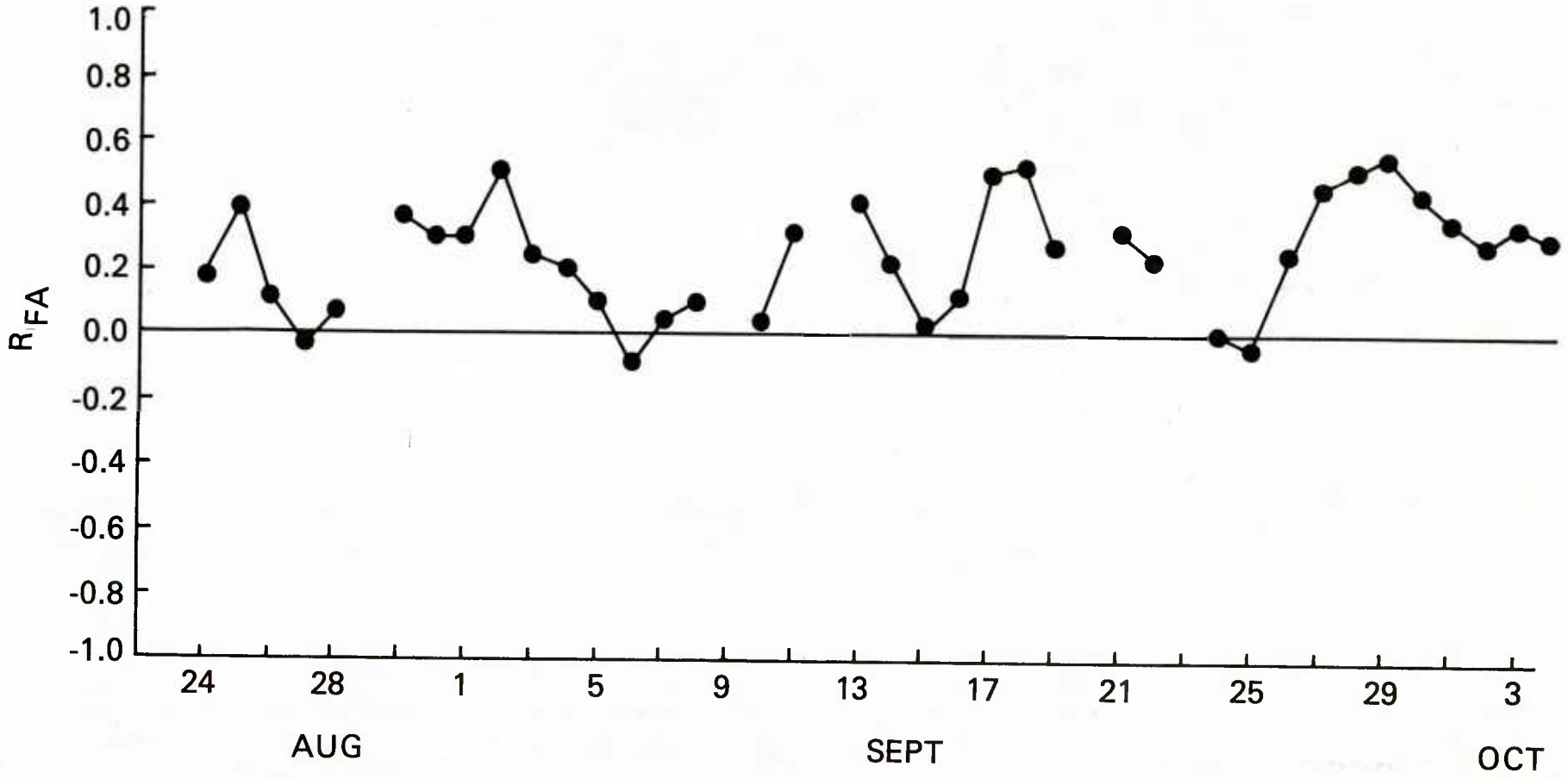

Figure 16(b). Same as 16(a) but for North Atlantic between 30° and 60°N, and 0° and 80°W.

We can proceed further with the correlation analysis formalism, however, and actually calculate R_{FT} and other quantities if we assume that the model neither consistently overpredicts nor consistently underpredicts changes in sea surface temperature. This implies

$$\overline{\Delta T_T \varepsilon_F} = 0 \tag{20}$$

which yields from (11) and (16)

$$R_{FA} = \frac{\overline{\Delta T_T \Delta T_T}}{\sigma_F \sigma_A} \tag{21}$$

Now, by definition

$$\overline{\Delta T_T \Delta T_T} = \sigma_T^2 \tag{22}$$

From this and (21) we have

$$R_{FA} = \frac{\sigma_T^2}{\sigma_F \sigma_A} \tag{23}$$

Using (23) to eliminate σ_T in (17) yields, after rearrangement,

$$R_{FT} = \left(\frac{\sigma_A}{\sigma_F} R_{FA} \right)^{1/2} \tag{24}$$

Figure 17 shows time series of R_{FT} calculated from (24) for the three-day changes in sea surface temperature predicted by the non-advective model during the fall 1980 test and evaluation program. The average value in the Pacific during this period was 0.65 (Figure 17(a)) while in the Atlantic it was 0.61 (Figure 17(b)). This is ample indication of skill in the forecast system.

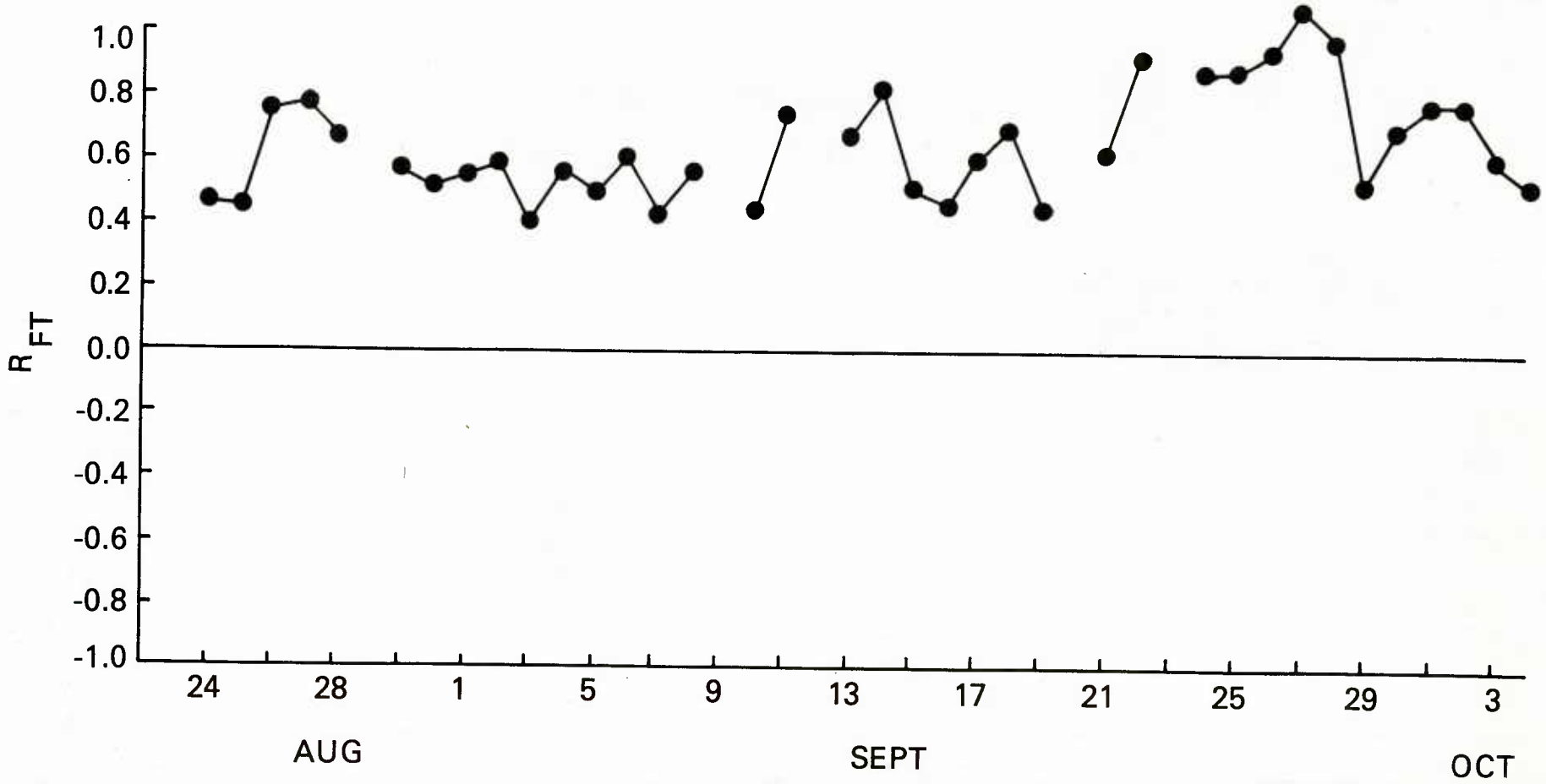

Figure 17(a). Same as 16(a) but for estimates of pattern correlations between forecast and true three-day changes in sea surface temperature calculated from equation 24.

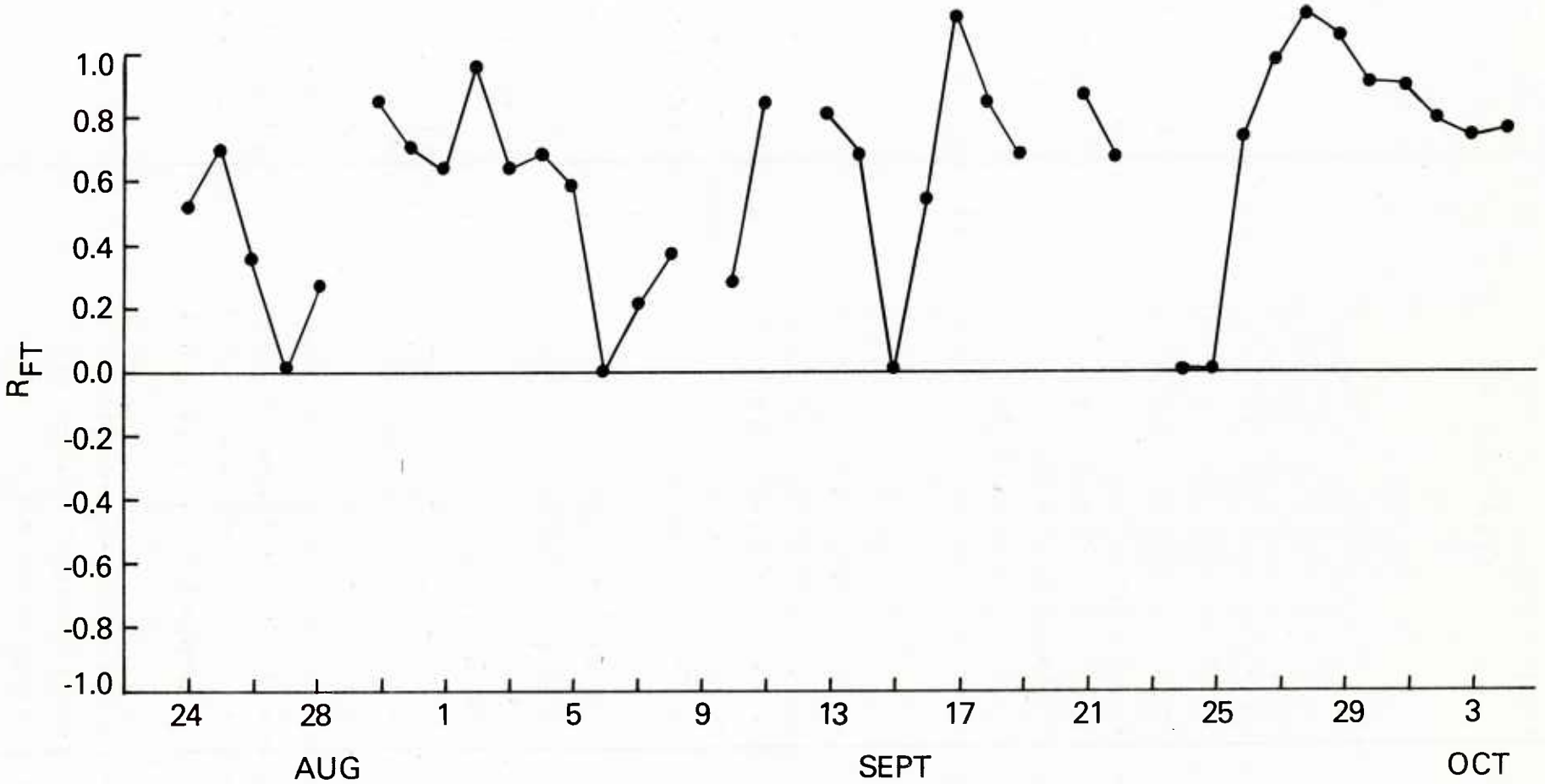

Figure 17(b). Same as 16(b) but for estimates of pattern correlations between forecast and true three-day changes in sea surface temperature calculated from equation 24. Note that R_{FT} is set to zero on this figure for cases in which $R_{FA} \leq 0$.

Another statistic of interest is the correlation between the analyzed and true temperature changes, R_{AT}. From equations (12), (15), and (23) we find

$$R_{AT} = \left(\frac{\sigma_F}{\sigma_A} R_{FA} \right)^{1/2} \qquad (25)$$

Figure 18 shows R_{AT} calculated from (25) and σ_T calculated from (23). Upon examination of this figure, a plausible and self-consistent interpretation of the temporal variability of R_{FA} and R_{FT} emerges. During periods of large change in the pattern of sea surface temperature, as evidenced by the relatively large values of σ_T, the quantities R_{AT}, R_{FT}, and R_{FA} tend to be relatively large. During periods when σ_T is small, implying little change in the pattern of sea surface temperature, the correlation coefficients all tend to be relatively small (see Figures 16, 17, and 18). This behavior is consistent with the concept of signal-to-noise ratio discussed earlier.

Comparison of Figures 17 and 18 produces another interesting fact: R_{FT} is typically 1.5-2 times as large as R_{AT}. This implies that TOPS gives a more accurate representation of changes in the pattern of sea surface temperature than the EOTS analysis does, on the time scale considered. This again emphasizes the potential advantages to be gained by using TOPS to supplement an ocean thermal analysis system.

In addition, we expect the skill of the model to be improved considerably when it is used to feed first-guess fields back into the ocean thermal analysis system that provides its initial conditions. Experience with TOPS has shown that on the three-day time scale, rapid model adjustment to spuriously shallow initial mixed-layer depths is a major source of forecast-change error. This situation is illustrated schematically in Figure 19. If the initial mixed-layer depth supplied to the model by EOTS is much shallower than the true mixed-layer depth, which is in near equilibrium with the surface forcing (as might be the case if the winds are anomalously high and no recent XBT observations are available nearby), the model rapidly deepens the mixed layer. This results in a spurious decrease in mixed-layer temperature as cold water is entrained into the layer from below.

When the model forecast is fed back into the analysis as a first-guess field, however, model physics rather than climatology will tend to control the mixed-layer depth in data-sparse regions. Thus, there will be a greater measure of

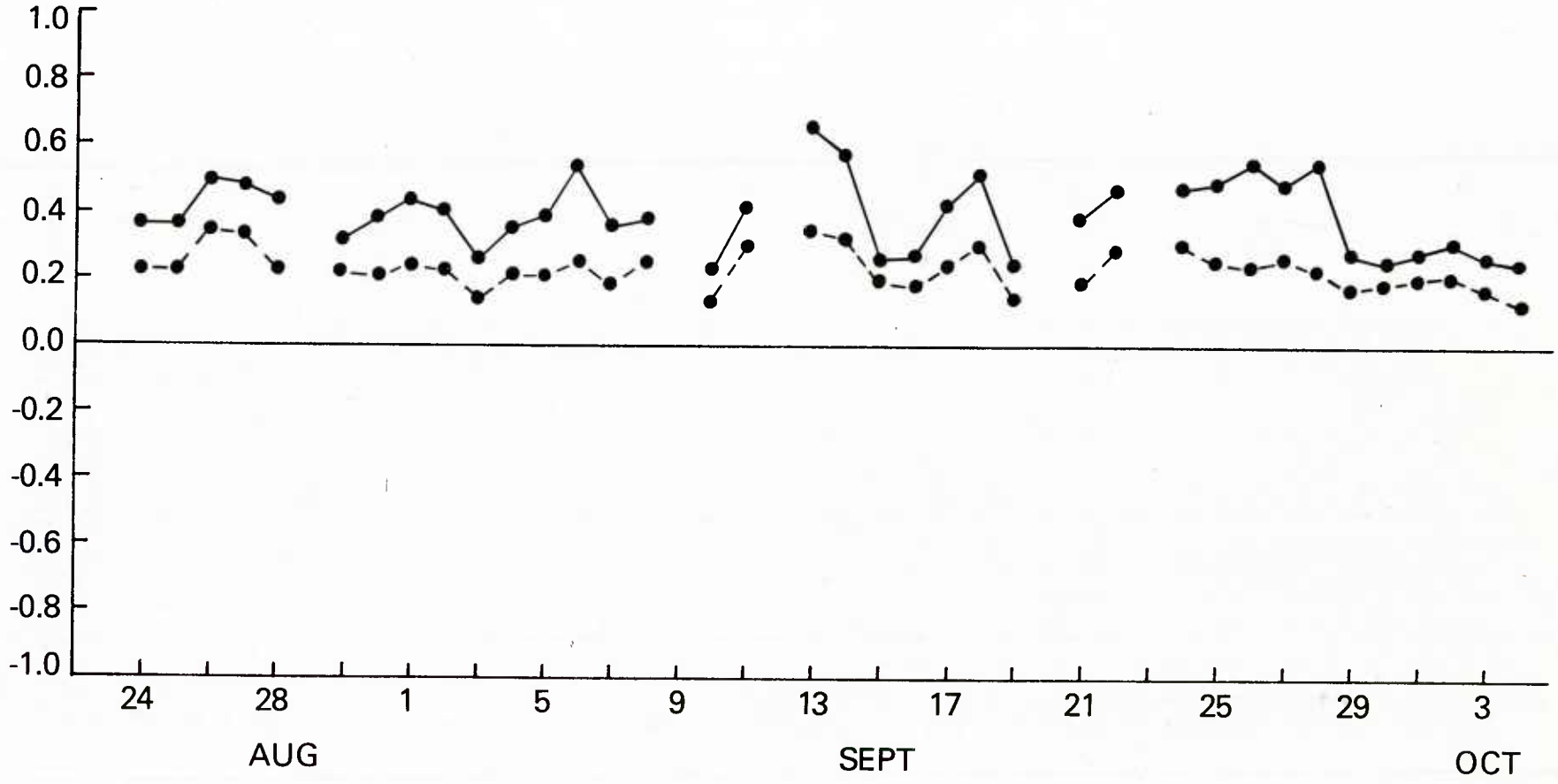

Figure 18(a). Estimates of R_{AT} (solid line, nondimensional) and σ_T (dashed line, °C) calculated from equations 23 and 25 in the North Pacific between 30° and 60°N, and 130°E and 115°W for a sequence of thirty-seven overlapping, three-day periods. Each data point is plotted on the day corresponding to the beginning of the relevant three-day period.

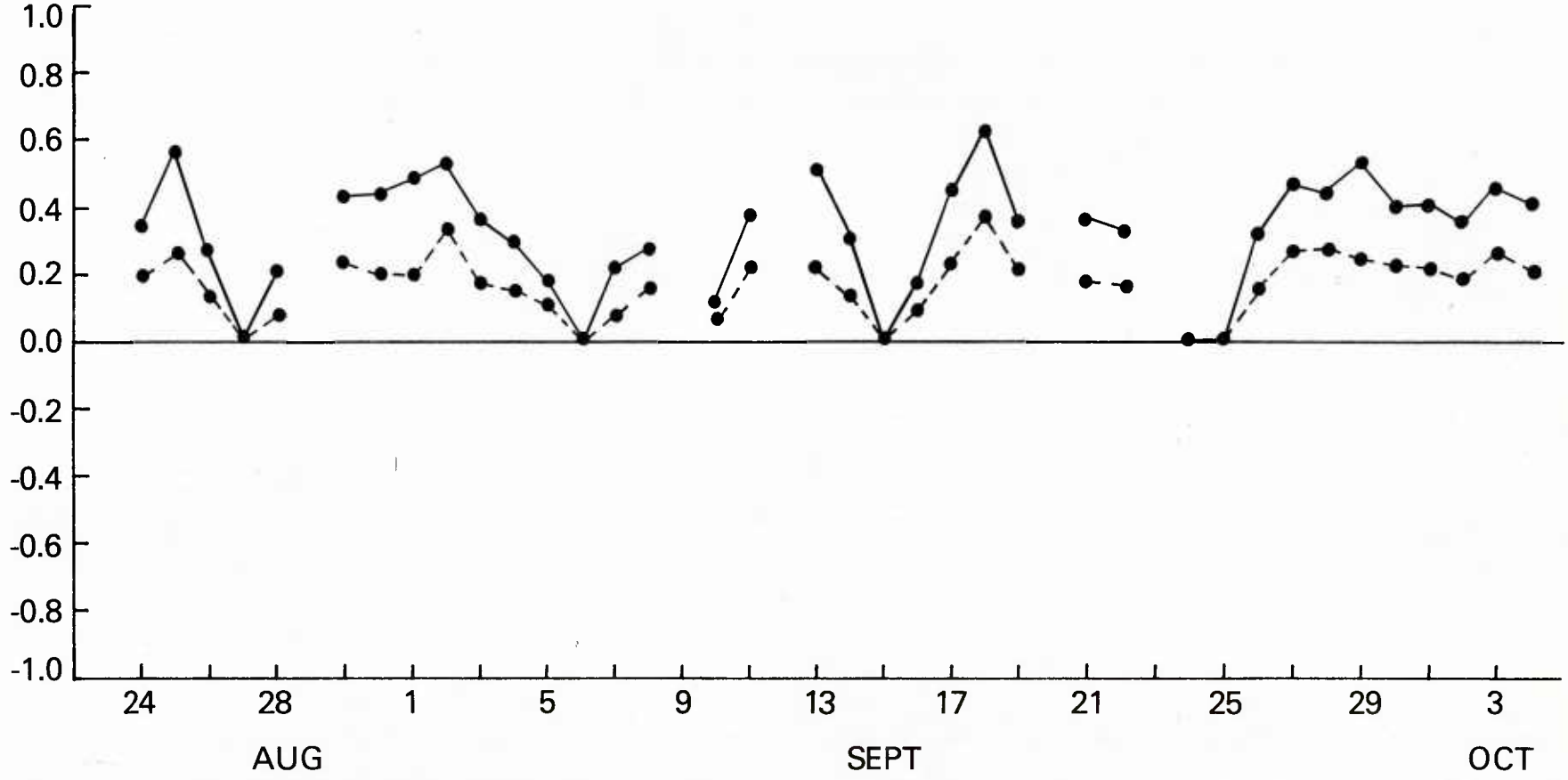

Figure 18(b). Same as 18(a) but for North Atlantic between 30° and 60°N, and 0° and 80°W. Note that R_{AT} and σ_T are set to zero in this figure for cases in which $R_{FA} \leq 0$.

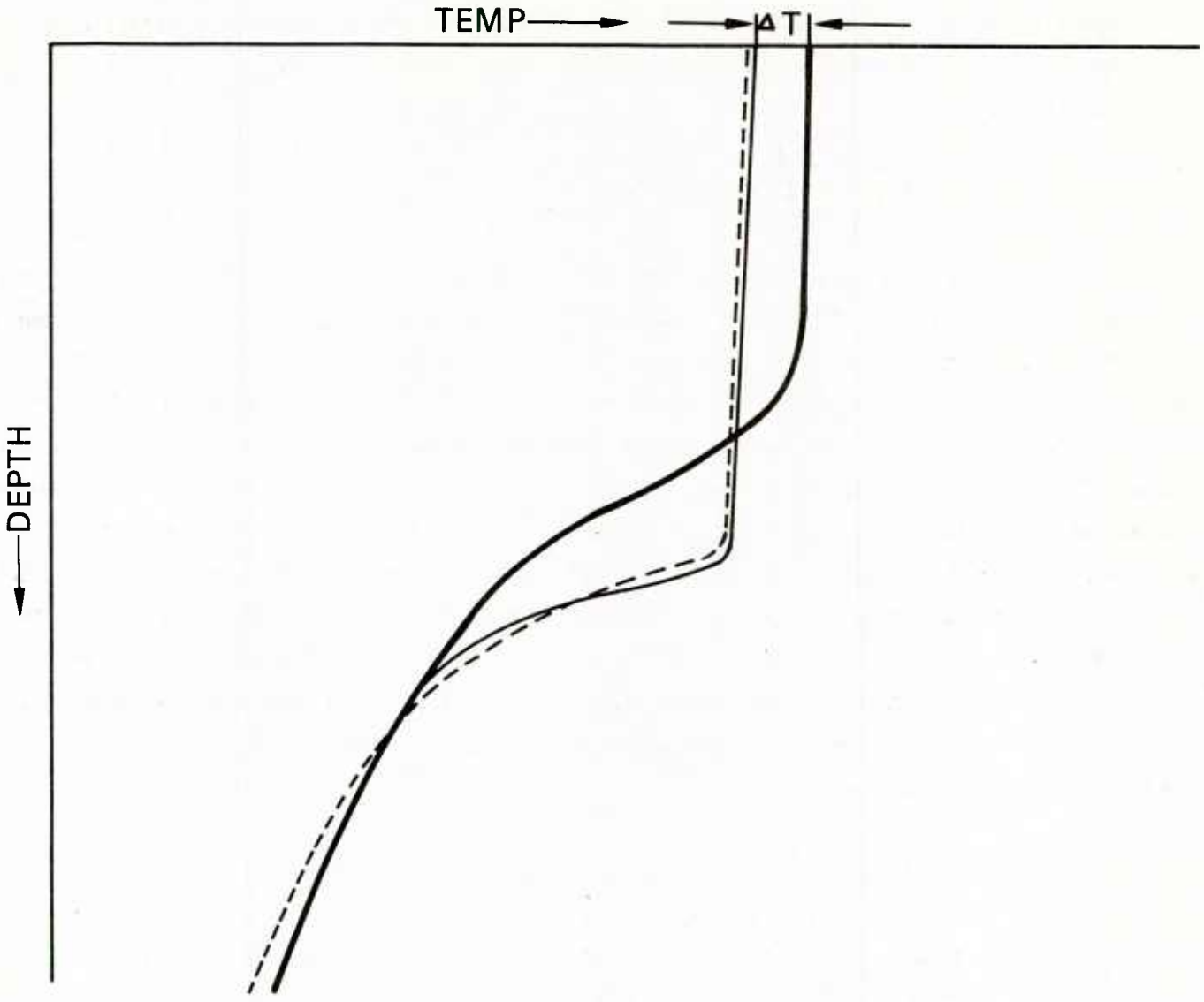

Figure 19. Schematic diagram illustrating rapid model adjustment to spuriously shallow initial mixed-layer depths. The heavy solid line is the initial temperature profile supplied to the model in a data-sparse region by the EOTS Analysis. The dashed line is the true initial temperature profile, which is in near equilibrium with the atmospheric forcing, and the thin solid line is the model temperature profile resulting after the initial adjustment of the mixed-layer depth. The quantity $\triangle T$ represents the spurious change in sea surface temperature caused by the initial adjustment process.

consistency between the analyzed mixed-layer depths and the local atmospheric forcing. This will greatly reduce the spurious changes in mixed-layer depth associated with the initial adjustment mechanism described above, and substantially increase the skill of the model in predicting short-term changes in sea surface temperature.

C. APPARENT FORECAST ERROR TECHNIQUE

Another useful strategy for short time scale synoptic verification of ocean thermal forecasts is to restrict attention to rather limited subareas characterized by strong atmospheric forcing in addition to adequate data coverage in an effort to achieve a better than usual signal (forecast change) to noise (error in verifying analysis) ratio. Then, statistics of the apparent model forecast error, which is simply the model-predicted temperature field minus the analyzed (i.e., EOTS) temperature field valid at the end of the forecast period, are computed. These statistics are subsequently compared to those of the apparent persistence forecast error, which is just the initial temperature field minus the analyzed temperature field valid at the end of the forecast period (both of which are supplied by EOTS), in an attempt to show that the model prediction is a significant improvement over persistence. This is the basic approach taken by Clancy and Martin (1981) in a case study of a three-day TOPS forecast.

We will apply this technique to the fall 1980 test and evaluation of the non-advective TOPS model. Eleven of the thirty-seven three-day forecasts produced during this period were examined and the three examples presented below were selected as being particularly interesting.

Figure 20 shows the surface atmospheric pressure analysis for the North Atlantic valid at 0Z 30 August 1980. With a minimum central pressure of 992 mb, the low pressure system immediately south of Greenland represents a moderately strong storm. During the three-day period following the map time, the largest sea surface temperature response predicted by TOPS occurred in the rectangular region shown on the figure, which is a 3 x 5 subset of the 63 x 63 model grid. Note that this region is also a relatively data-rich area since it is traversed by most of the shipping lanes which link Europe with the East Coast of the United States.

Figure 21 shows the root-mean-square (RMS) apparent sea surface temperature forecast errors in the rectangular region resulting from three-day persistence and

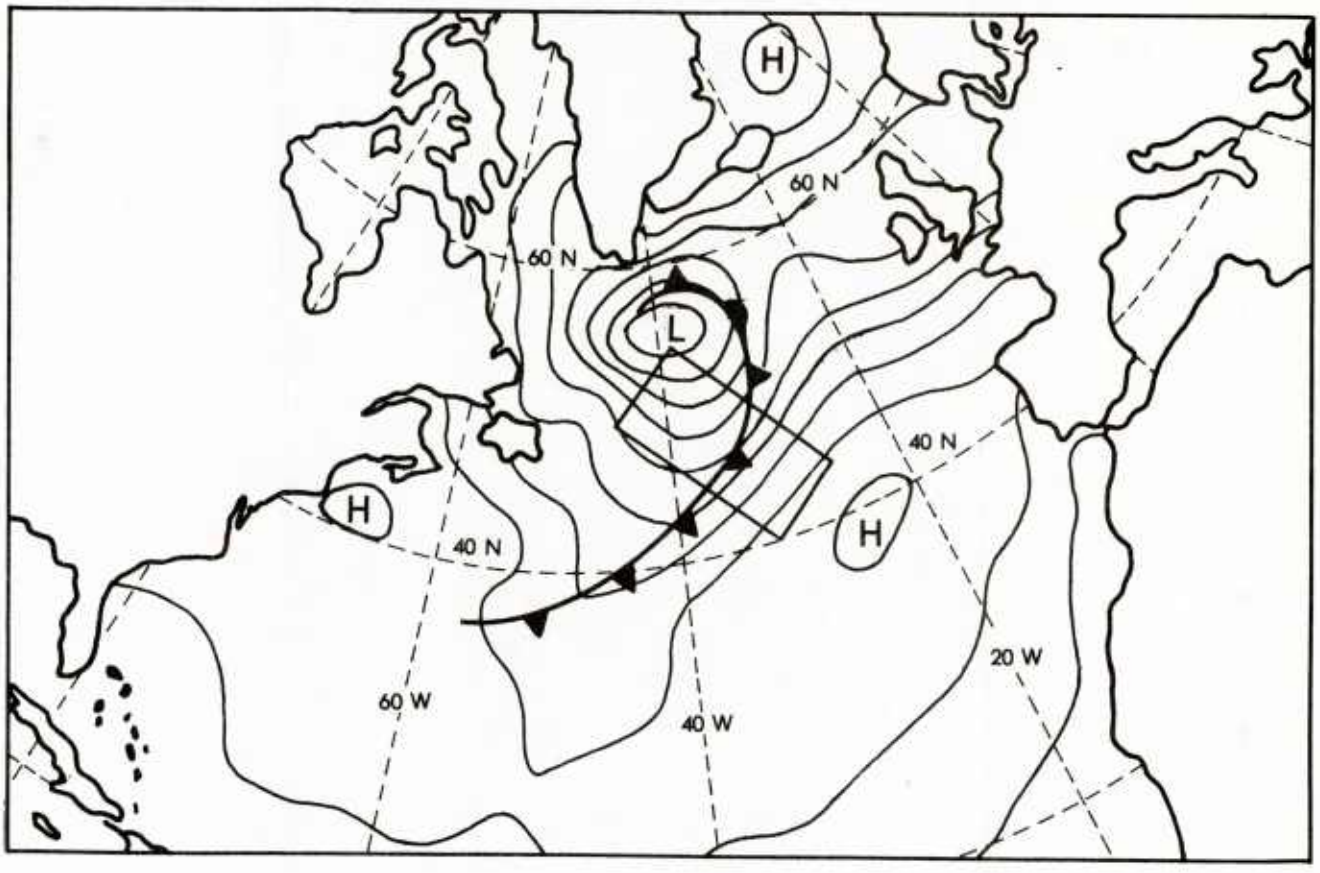

Figure 20. Surface pressure analysis for the North Atlantic at 0Z 30 August 1980. The contour interval is 4mb and the interior contour of the low corresponds to 992mb. The rectangular box is a 3 x 5 subset of the 63 x 63 model grid in which verification statistics are computed.

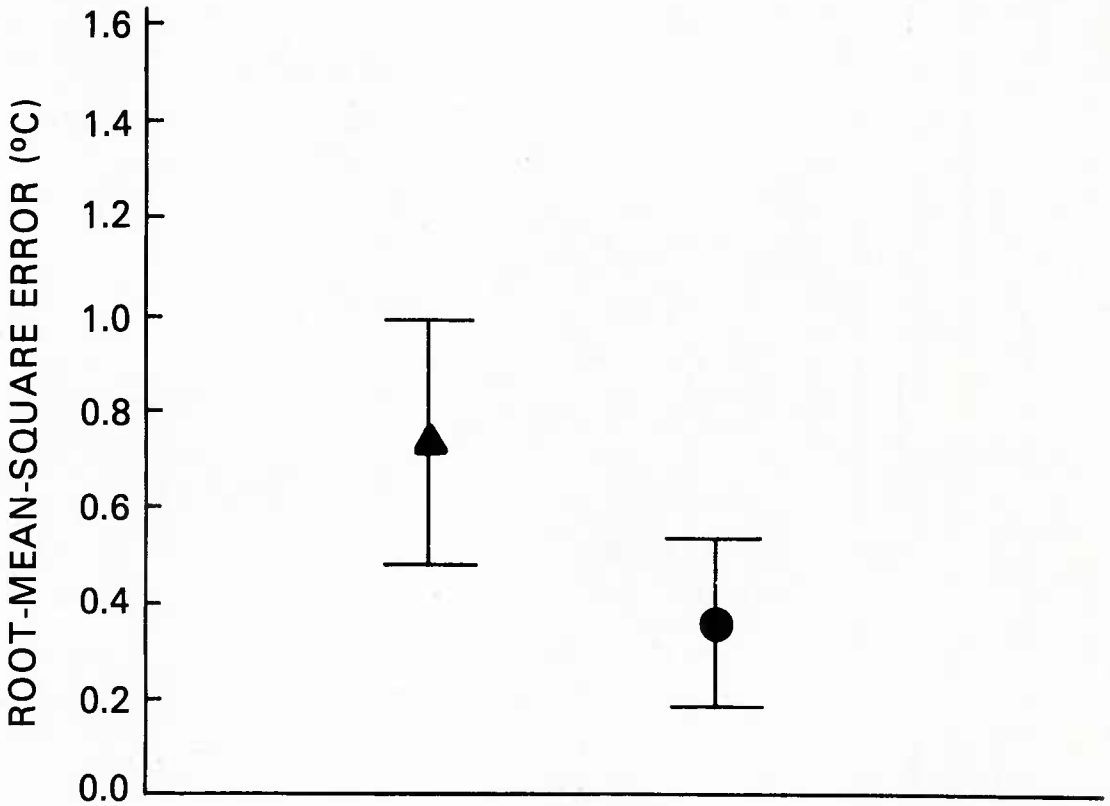

Figure 21. Root-mean-square apparent forecast errors for three-day persistence (▲) and model (●) forecasts of sea surface temperature from 0Z 30 August 1980 in the rectangular box shown in Figure 20. The error bars represent 95% confidence limits for the true root-mean-square errors.

model forecasts from OZ 30 August. The error bars represent 95% confidence limits on the true RMS errors based on the assumption that the apparent forecast errors are normally distributed about the true errors. As can be seen from the figure, the RMS apparent persistence forecast error is approximately twice that of the model.

Another interesting example is afforded by Figure 22 which shows the surface atmospheric pressure analysis for the Central North Pacific at OZ 28 September 1980. The low pressure system prominent in the figure was the first major storm of the season to move across the Pacific; at the time shown, its minimum central pressure was 972 mb. During the three-day period following the map time, the strongest thermal response predicted by the model occurred in the rectangular region shown in the figure, which is a 6 x 10 subset of the model grid. As before, the selected subarea is characterized by relatively good data coverage which is, in this case, due primarily to shipping traffic between the West Coast of the United States and Japan.

The RMS apparent sea surface temperature errors in the rectangular subarea for three-day persistence and model forecasts for this case are shown in Figure 23. Again, as indicated by the figure, the RMS persistence error is approximately twice that of the model. Note that the confidence intervals are smaller in this example because of the higher degree of statistical certainty associated with the larger number of gridpoints in the selected subarea.

Finally, in Figure 24 we see the surface pressure analysis for the Western North Pacific at OZ 29 September. The weather pattern of interest in this figure is the low pressure system southeast of Japan which is, in fact, tropical storm Thelma with a central pressure of 992 mb. During the period of interest, the storm moved to the northeast. Once again we indicate the region in which we calculate verification statistics with a rectangle on the figure and note that it is characterized by better than average data coverage. In this case, the data coverage is due primarily to shipping traffic between Japan and Hawaii, Australia, and Southeast Asia.

Figure 25 shows the RMS apparent sea surface temperature errors for three-day persistence and model forecasts for this case. As before, the model forecast betters persistence by a factor of about two.

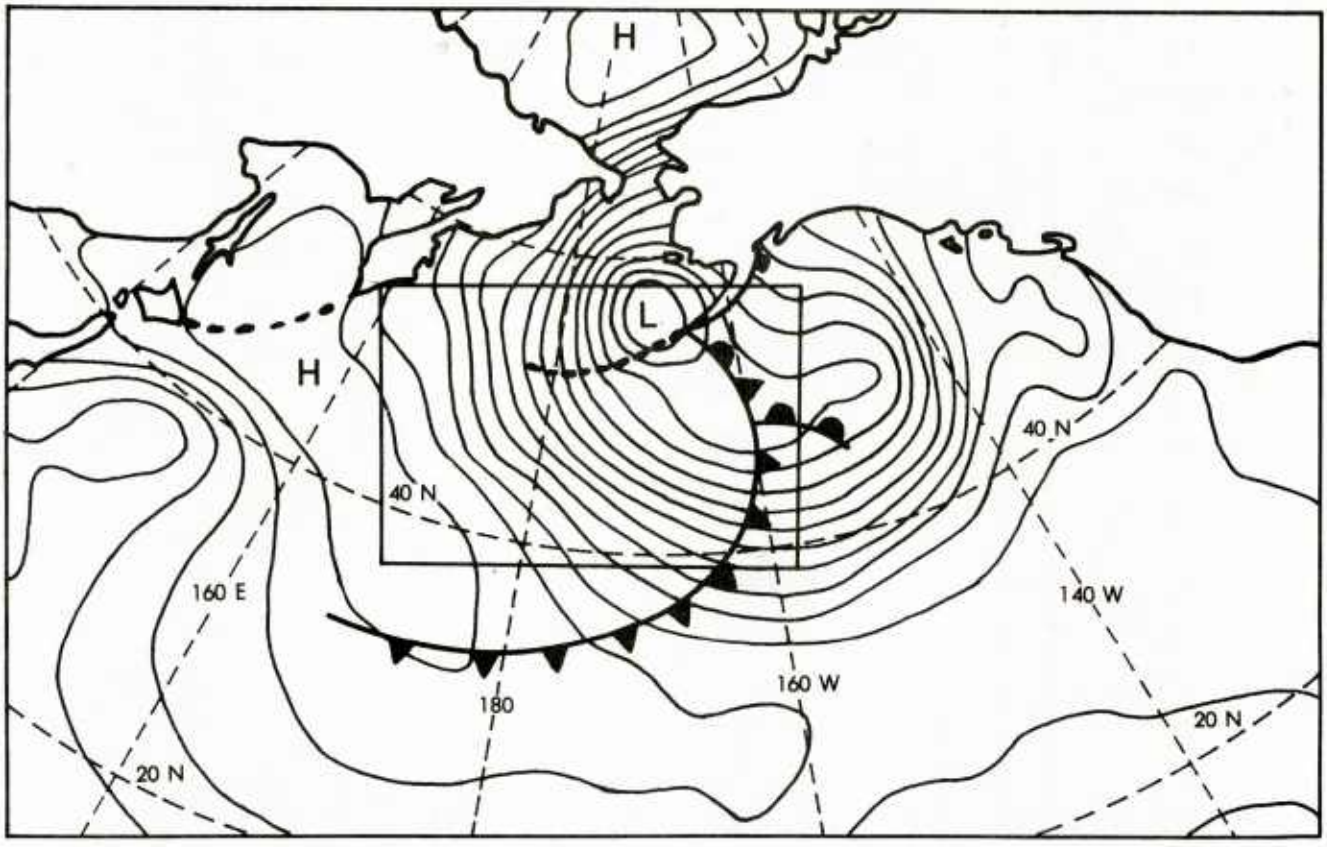

Figure 22. Surface pressure analysis for the Central North Pacific at 0Z 28 September 1980. The contour interval is 4mb and the interior contour of the low corresponds to 972mb. The rectangular box is a 6 x 10 subset of the 63 x 63 model grid in which verification statistics are computed.

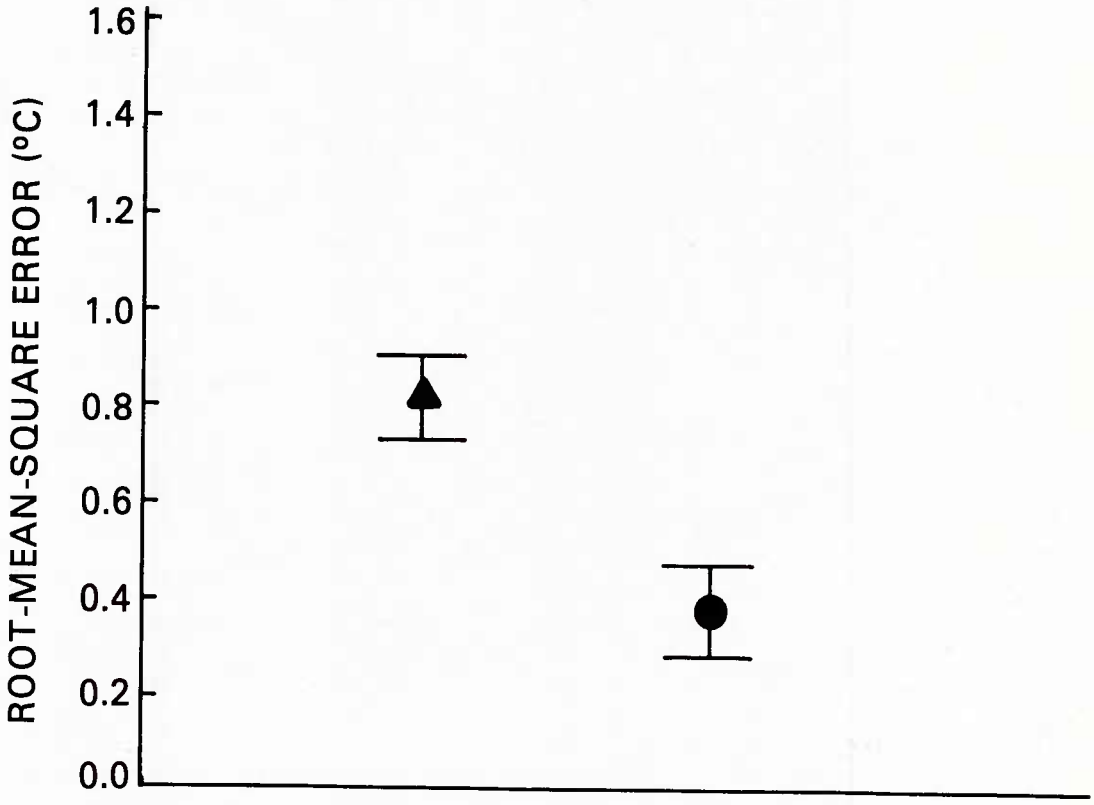

Figure 23. Same as Figure 21 but for three-day persistence (▲) and model (●) forecasts from 0Z 28 September 1980 in the rectangular box shown in Figure 22.

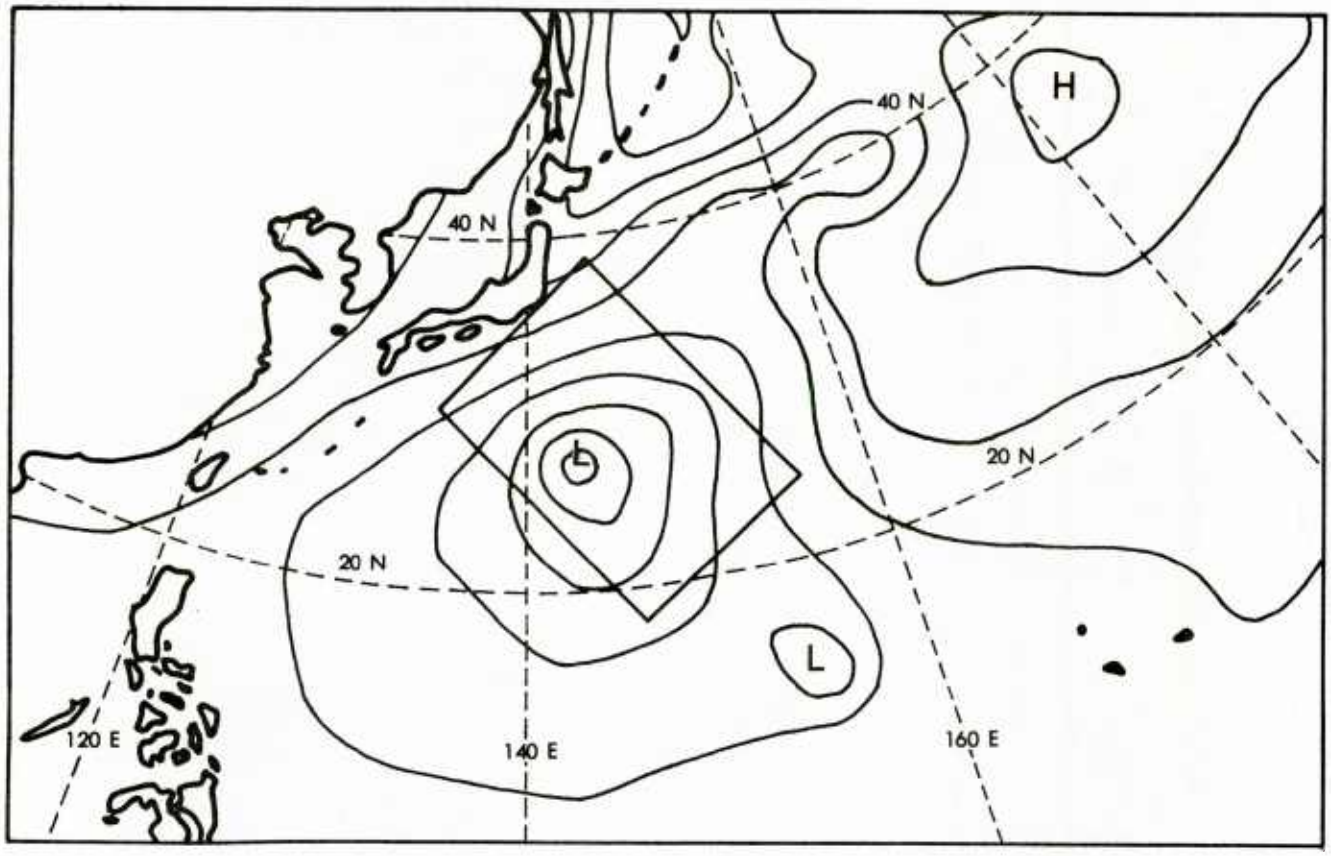

Figure 24. Surface pressure analysis for the Western North Pacific at 0Z 29 September 1980. The contour interval is 4mb and the interior contour of the low immediately southeast of Japan corresponds to 992mb. The rectangular box is a 6 x 5 subset of the 63 x 63 model grid in which verification statistics are computed.

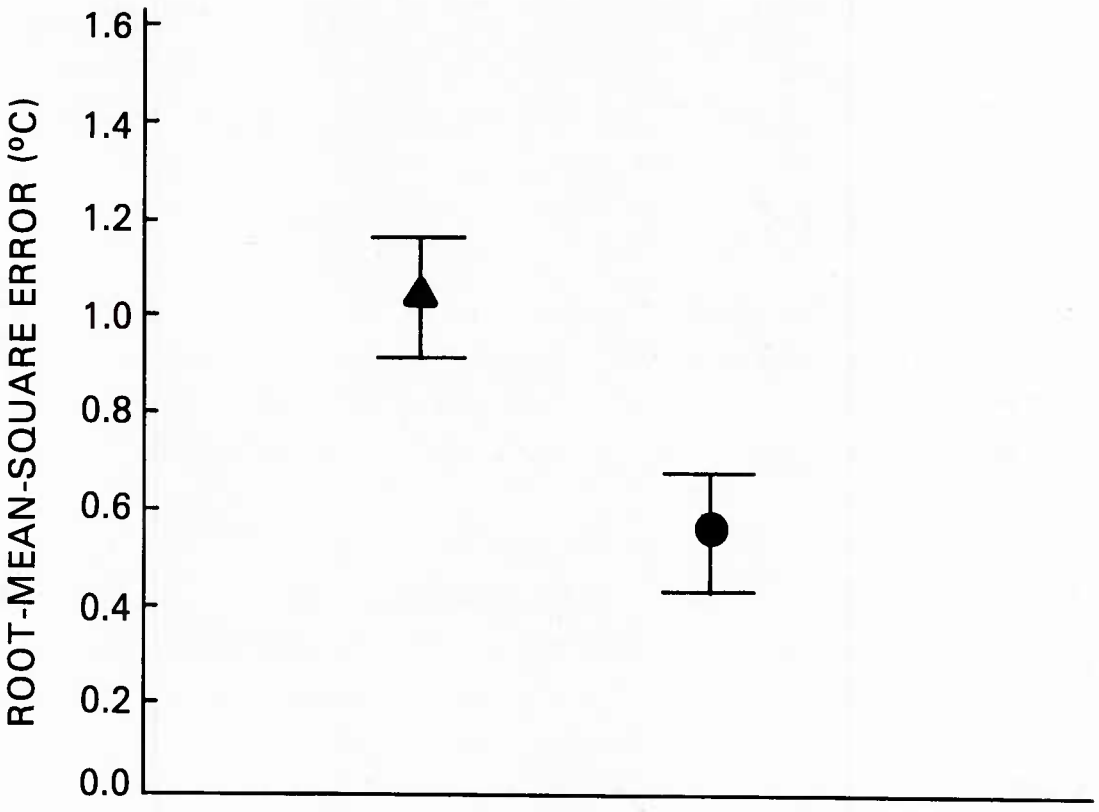

Figure 25. Same as Figure 21 but for three-day persistence (▲) and model (●) forecasts from 0Z 29 September 1980 in the rectangular box shown in Figure 24.

The results shown in Figures 21, 23, and 25 are fairly typical of verification statistics obtained for regions of strong atmospheric forcing and adequate data coverage. In regions of weak atmospheric forcing, of course, the improvement of the model forecast over persistence is not as great. Finally, we note that in cases of strong atmospheric forcing occurring in data-void regions, the model forecast will appear worse than persistence since the EOTS analysis will simply track along the slowly varying climatological trend while TOPS will predict a rapid change. Consequently, this method of forecast verification must be applied carefully.

V. SUMMARY AND OUTLOOK

The Thermodynamical Ocean Prediction System (TOPS) is a flexible software framework for operational implementation of synoptic ocean mixed-layer models at Fleet Numerical Oceanography Center (FNOC). It was developed by the Naval Ocean Research and Development Activity (NORDA) as a part of the Navy's Automated Environmental Prediction System.

In this paper we have described the first generation of models implemented via TOPS and discussed the potential uses for their output products. We have also developed a formalism, based on the pattern-of-change correlation technique, for verification of three-day time scale synoptic upper ocean thermal forecasts and used this formalism to analyze model predictions from the fall of 1980. The results of this analysis demonstrate that TOPS is capable of routinely producing useful real-time forecasts of large-scale changes in sea surface temperature. In addition, we have compared the apparent forecast errors (forecast field minus verifying analysis) for sea surface temperature resulting from three-day model forecasts to those due to persistence (i.e., a forecast of no change over the three-day period) for several cases. In limited regions of strong atmospheric forcing and adequate data coverage, the skill of the model, as measured by the root-mean-square apparent forecast error, is typically twice that of persistence.

The fact that TOPS can produce skillfull forecasts is not surprising. The turbulence parameterization model currently used has been tested favorably in a number of one-dimensional studies, as have the FNOC atmospheric forcing fields which drive TOPS. Nevertheless, demonstration of this skill is a significant achievement since it marks the practical beginning of operational synoptic ocean prediction.

As discussed in Section III, one of the most important applications for TOPS is to generate first-guess thermal fields for the ocean thermal analysis system that provides the prediction model with its initial conditions. Feeding the model forecast back into the analysis will tend to make the analyzed thermal fields dynamically consistent with the atmospheric forcing of the ocean, and efforts are currently underway to couple TOPS and the EOTS analysis in this manner.

When TOPS is used to feed first-guess thermal fields back into an ocean thermal analysis system, the model prediction may be carried along for months in a data-sparse region before being updated with observations. Thus, the model must verify on much longer time scales than what was considered here.

For long time scale integrations of TOPS, the accuracy of the atmospheric forcing fields used to drive the ocean model become a critical consideration. Elsberry et al. (1979) show evidence suggesting the existence of significant biases in the net surface heat flux obtained from the FNOC fields for certain regions. Because of the highly nonlinear aspect of the heating/mixing process in the upper ocean, such biases could have disasterous effects on the model solution after a period of several months. As a result, suitably accurate surface heat fluxes are a key element in comprehensive ocean analysis/prediction. Thus, the forcing fields generated by the Naval Operational Global Atmospheric Prediction System (NOGAPS) model, which will probably replace the existing FNOC atmospheric PE model in the near future, will have to be scrutinized carefully.

Three additional operational ocean products will be produced for FNOC by NORDA over the next several years: (1) a world ocean primitive equation model, (2) an improved ocean thermal analysis system, and (3) a search and rescue model. TOPS will be coupled to all of these products.

The world ocean primitive equation model will be a global, layer-averaged model with two or three layers and horizontal grid spacing on the order of 50 km. It will include a simplified treatment of thermodynamics (e.g., Clancy et al., 1979). In the first operational applications of this model, however, it will not be updated with ocean thermal observations. Instead, it will be spun up to the present point in time with historical atmospheric forcing and then simply integrated forward day-by-day with the observed atmospheric data. This type of model should provide a good representation of the mean large-scale ocean circulation and the statistics of the eddy field (e.g., Hurlburt and Thompson, 1976; Hurlburt and Thompson, 1980).

It will be used to supply the geostrophic component of the advection current to TOPS. Thus, the approach we take in designing a comprehensive ocean prediction system is to treat hydrodynamical processes with minimum vertical resolution and maximum horizontal resolution (world ocean model) while retaining a thermodynamical model with high vertical resolution but low horizontal resolution (TOPS) in order to provide meaningful input to acoustic models.

The improved ocean thermal analysis system will be an objective analysis scheme based on the optimum interpolation technique (e.g., White and Bernstein, 1979). It will be designed to make maximum use of satellite data which will be combined with the traditional observations in a statistically optimum way. TOPS will be used to generate the first-guess fields for this system, and it will be advanced as a replacement for the EOTS analysis.

Finally, the search and rescue model will be a system that takes output from TOPS and the world ocean model, along with other environmental information, to predict the drift of life rafts and/or wreckage on the open ocean. It will replace an existing FNOC product and will be run only as a result of special requests.

It is anticipated that important contributions to our basic understanding of variability in the upper ocean will be made by many research groups in the decade ahead. The advances produced by basic research will quickly find their way into TOPS (in the form of improved turbulence models, better analysis techniques, etc.) with the net result that the Navy's operational ocean prediction capabilities will be steadily improved.

VI. REFERENCES

Barnett, T. P., D. R. McLain, S. E. Larson, and E. J. Steiner (1980). Comparison of Various Sea Surface Temperature Fields. COSPAR/SCOR/IUCRM Symposium on Oceanography from Space, Venice, Italy, May, 11 p.

Bergman, K. (1979). Multivariate Analysis of Temperature and Winds Using Optimum Interpolation. Mon. Wea. Rev.,107, 1423-1444.

Camp, N. T. and R. L. Elsberry (1978). Oceanic Thermal Response to Strong Atmospheric Forcing II. The Role of One-Dimensional Processes. J. Phys. Oceanog., 8, 215-224.

Clancy, R. M., J. D. Thompson, H. E. Hurlburt, and J. D. Lee (1979). A Model of Mesoscale Air-Sea Interaction in a Sea Breeze-Coastal Upwelling Regime. Mon. Wea. Rev., 107, 1476-1505.

Clancy, R. M. (1979). A Model of Diurnal Variability of the Ocean-Atmosphere System in the Undisturbed Trade Wind Regime. Tech. Report SAI-79-807-WA, Science Applications, Inc., 17109 Goodridge Drive, McLean, VA, July, 114 p.

Clancy, R. M. and P. J. Martin (1979). The NORDA/FLENUMOCEANCEN Thermodynamical Ocean Prediction System (TOPS): A Technical Description. NORDA Technical Note 54, Naval Ocean Research and Development Activity, NSTL Station, MS, November, 28 p.

Clancy, R. M. and P. J. Martin (1981). Synoptic Forecasting of the Oceanic Mixed Layer Using the Navy's Operational Environmental Data Base: Present Capabilities and Future Applications. (To appear in the June issue of Bulletin of the American Meteorological Society).

Clancy, R. M. (1981). A Note on Finite Differencing of the Advection-Diffusion Equation. (To appear in Monthly Weather Review).

Dobryshman, E. M. (1972). Review of Forecast Verification Techniques. WMO Technical Note 120, World Meteorological Organization, Geneva, Switzerland, 51 p.

Dunlap, C. R. and G. P. Tierney (1981). Fleet Acoustic Prediction Systems: Where Are We? Proc. U. S. Naval Institute, 107/1/935, 98-100.

Elsberry, R. L. and N. T. Camp (1978). Oceanic Thermal Response to Strong Atmospheric Forcing I. Characteristics of Forcing Events. J. Phys. Oceanog., 8, 206-214.

Elsberry, R. L. and S. D. Raney (1978). Sea Surface Temperature Response to Variations in Atmospheric Wind Forcing. J. Phys. Oceanog., 8, 881-887.

Elsberry, R. L. and R. W. Garwood (1978). Sea Surface Temperature Anomaly Generation in Relation to Atmospheric Storms. Bull. Am. Meteorol. Soc., 49, 786-789.

Elsberry, R. L., P. C. Gallacher, and R. W. Garwood (1979). One-Dimensional Model Predictions of Ocean Temperature Anomalies During Fall 1976. Tech. Report NPS 63-79-003, Naval Postgraduate School, Monterey, CA, August, 30 p.

Garwood, R. W. (1977). An Oceanic Mixed Layer Model Capable of Simulating Cyclic States. J. Phy. Oceanog., 7, 455-468.

Haney, R. L. (1974). A Numerical Study of the Response of an Idealized Ocean to Large-Scale Surface Heat and Momentum Flux. J. Phy. Oceanog., 4, 145-167.

Haney, R. L. (1980). A Numerical Case Study of the Development of Large-Scale Thermal Anomalies in the Central North Pacific Ocean. J. Phys. Oceanog., 10, 541-566.

Holl, M. M., M. J. Cuming, and B. R. Mendenhall (1979). The Expanded Ocean Thermal Structure Analysis System: A Development Based on the Fields by Information Blending Methodology. Tech. Report M-241, Meteorology International, Incorporated, 2600 Garden Road, Suite 145, Monterey, CA, 216 p.

Hurlburt, H. E. and J. D. Thompson (1976). A Numerical Model of the Somali Current. J. Phys. Oceanog., 6, 646-664.

Hurlburt, H. E. and J. D. Thompscn (1980). A Numerical Study of Loop Current Intrusions and Eddy Shedding. J. Phys. Oceanog., 10, 1611-1651.

Kesel, P. G. and F. J. Winningoff (1972). The Fleet Numerical Weather Central Operational Primitive-Equation Model. Mon. Wea. Rev., 100, 360-373.

Kirwan, A. D., N. L. Guinasso, and G. McNally (1978). Sea Surface Temperatures in the North Pacific Through the Winter of 1976-1977 from Nimbus 6. J. Geophys. Res., 83, 5505-5506.

Martin, P. J. (1976). A Comparison of Three Diffusion Models of the Upper Mixed-Layer of the Ocean. NRL Memorandum Report 3399, Naval Research Laboratory, Washington, D.C., November, 53 p.

Martin, P. J. (1981). Numerical Simulation of Upper Ocean Response to Hurricane Eloise. (Submitted to Journal of Physical Oceanography).

Martin, P. J. and J. D. Thompson (1981). Formulation and Testing of a Layer-Compatible Upper Ocean Mixed-Layer Model. (Submitted to Journal of Geophysical Research).

McPherson, R. D., K. H. Bergman, R. E. Kistler, G. E. Rasch, and D. S. Gordon (1979). The NMC Operational Global Data Assimilation System. Mon. Wea. Rev., 107, 1445-1461.

Mellor, G. L. and T. Yamada (1974). A Hierarchy of Turbulence Closure Models for Planetary Boundary Layers. J. Atmos. Sci., 31, 1791-1806.

Mellor, G. L. and P. A Durbin (1975). The Structure and Dynamics of the Ocean Surface Mixed-Layer. J. Phys. Oceanog., 5, 718-725.

Mendenhall, B. R., M. J. Cuming and M. M. Holl (1978). The Expanded Ocean Thermal-Structure Analysis System Users Manual. Tech. Report M-232, Meteorology International Incorporated, 2600 Garden Road, Suite 145, Monterey, CA, 110 p.

Mihok, W. F., and J. E. Kaitala (1976). U. S. Navy Fleet Numerical Weather Central Operational Five-Level Global Fourth-Order Primitive-Equation Model. Mon. Wea. Rev.,104, 1527-1550.

Miller, J. R. (1976). The Salinity Effect in a Mixed-Layer Model. J. Phys. Oceanog., 6, 29-35.

Naval Air Systems Command (1978). U. S. Naval Weather Service Numerical Environmental Products Manual. Technical Report NAVAIR 50-1G-522, CNOC, NSTL Station, MS.

Niiler, P. P. and E. B. Kraus (1977). One-Dimensional Models of the Upper Ocean. Chapt. 10, Modelling and Prediction of the Upper Layers of the Ocean. New York, Pergamon Press, 325 p. (Pergamon Marine Series, v. 1).

Pollard, R. T. and R. C. Millard (1970). Comparison Between Observed and Simulated Wind-Generated Inertial Oscillations. Deep Sea Res., 17, 813-821.

Pollard, R. T., P. B. Rhines, and R. O. Thompson (1973). The Deepening of the Wind Mixed Layer. Geophy. Fluid Dyn., 3, 381-404.

Price, J. F., C. N. K. Mooers, and J. C. Van Leer (1978). Observations and Simulation of Storm-Induced Mixed-Layer Deepening, J. Phys. Oceanog., 8, 582-599.

Price, J. F. (1979). Observations of a Rain-Formed Mixed Layer. J. Phys. Oceanog., 9, 643-649.

Price, J. F. (1981). On The Upper Ocean Response to a Moving Hurricane. (Submitted to Journal of Physical Oceanography).

Shonting, D. H. (1964). Observations of Short Term Heating of the Surface Layer of the Ocean. Technical Memorandum No. 308, U. S. Naval Underwater Ordnance Station, Newport, RI, 22 p.

Strong, A. E. and J. A. Pritchard (1980). Regular Monthly Mean Temperatures of Earth's Oceans from Satellites. Bull. Am. Meteorol. Soc., 61, 553-559.

Thompson, R. O. (1976). Climatological Numerical Models of the Surface Mixed Layer of the Ocean. J. Phys. Oceanog., 6, 496-503.

Urick, R. J. (1975). Principles of Underwater Sound, Chapt. 1, New York, McGraw-Hill, Inc., 384 p.

Vager, B. G. and S. S. Zilitinkevich (1968). A Theoretical Model of Diurnal Variations of the Meteorological Fields. Meteorol. I. Girdrol, 7.

Warn-Varnas, A. C. and S. A. Piacsek (1979). An Investigation of the Importance of Third-Order Correlations and Choice of Length Scale in Mixed-Layer Modeling. Geophys. Astrophys. Fluid Dyn., 13, 225-243.

Warn-Varnas, A. C., G. M. Dawson, and P. J. Martin (1981). Forecasts and Studies of the Oceanic Mixed Layer During the MILE Experiment. Geophys. Astrophys. Fluid Dyn., 16, 1-23.

Warn-Varnas, A. C. and G. M. Dawson (1981). An Analysis of Modelled Shear Distribution During MILE. NORDA Technical Note 84, Naval Ocean Research and Development Activity, NSTL Station, MS, February, 36 p.

Weigle, W. F. and B. R. Mendenhall (1974). Climatology of the Upper Thermal Structure of the Seas. Tech. Report M-196, Meteorology International, Incorporated, 2600 Garden Road, Suite 145, Monterey, CA, 79 p.

White, W. B. and R. L. Bernstein (1979). Design of an Oceanographic Network in the Midlatitude North Pacific. J. Phys. Oceanog., 9, 592-606.

World Meteorological Organization (1977). Integrated Global Ocean Station System-General Plan and Implementation Programme 1977-1982. Tech. Report WMO No. 466, 37 p.

Yamada, T. (1979). PBL Similarity Profiles Determined from a Level-2 Turbulence-Closure Model. Boundary Layer Met., 17, 333-351.

APPENDIX

LIST OF SYMBOLS

SYMBOL	DEFINITION
A	Horizontal eddy diffusion coefficient
c	Specific heat of seawater
D	Damping coefficient for inertial oscillations
F	Downward flux of solar radiation
f	Coriolis parameter
R_{AT}	Correlation between the analyzed and true temperature changes
R_{FA}	Correlation between the forecast and analyzed temperature changes
R_{FT}	Correlation between the forecast and true temperature changes
S	Salinity
t	Time
T	Temperature
u	x-component of current velocity
u_i	x-component of instantaneous Ekman plus inertial part of advection current
u_g^*	x-component of divergence-free geostrophic part of advection current

u_a	x-component of advection current
v	y-component of current velocity
v_i	y-component of instantaneous Ekman plus inertial part of advection current
v_g^*	y-component of divergence-free geostrophic part of advection current
v_a	y-component of advection current
w	z-component of current velocity
w_i	z-component of current velocity due to divergence of u_i and v_i
w_a	z-component of advection current
x	Grid-referenced horizontal coordinate
y	Grid-referenced horizontal coordinate
z	Vertical coordinate, positive upward from sea surface
$(\overline{\quad})$	Ensemble mean for equations (1)-(6). Average over gridpoints in a specified region for equations (10)-(22)
$(')$	Departures from above-defined averages
ΔT_F	Forecast change in ensemble-mean temperature
ΔT_A	Analyzed change in ensemble-mean temperature
ΔT_T	True change in ensemble-mean temperature
ε_F	Error in forecast ensemble-mean temperature change

ε_A	Error in analyzed ensemble-mean temperature change
σ_F	Standard deviation of ΔT_F
σ_A	Standard deviation of ΔT_A
σ_T	Standard deviation of ΔT_T
$\sigma_{A\varepsilon}$	Standard deviation of ε_A
ν	Background vertical eddy diffusion coefficient
ρ_w	Reference density for water